SEPSIS INDUCES DEREGULATION OF IL-13 PRODUCTION AND PD-1 EXPRESSION IN LUNG GROUP 2 INNATE LYMPHOID CELLS

Yuichi Akama,[*†] Eun Jeong Park,[*] Naoko Satoh-Takayama,[‡§] Arong Gaowa,[*]
Atsushi Ito,[*‖] Eiji Kawamoto,[*†] Samuel Darkwah,[*] Michael G. Appiah,[*]
Phyoe Kyawe Myint,[*] Hiroshi Ohno,[‡§¶] Hiroshi Imai,[†] and Motomu Shimaoka[*]

*Department of Molecular Pathobiology and Cell Adhesion Biology, Mie University Graduate School of Medicine, Tsu City, Mie, Japan; †Department of Emergency and Disaster Medicine, Mie University Graduate School of Medicine, Tsu City, Mie, Japan; ‡Laboratory for Intestinal Ecosystem, Center for Integrative Medical Sciences, RIKEN, Tsurumi-ku, Yokohama, Kanagawa, Japan; §Immunobiology Laboratory, Graduate School of Medical Life Science, Yokohama City University, Tsurumi-ku, Yokohama, Kanagawa, Japan; ‖Department of Thoracic and Cardiovascular Surgery, Mie University Graduate School of Medicine, Tsu City, Mie, Japan; and ¶Intestinal Microbiota Project, Kanagawa Institute of Industrial Science and Technology, Kawasaki, Kanagawa, Japan

ABSTRACT—Deregulation of the immune system in sepsis plays the central role in the pathogenesis of multiple organ failure including septic lung injury. Group 2 innate lymphoid cells (ILC2s) have emerged as a new player in regulating immune homeostasis in the lung; however, the role of ILC2s in lung injury in sepsis remains poorly understood. Here, we investigated temporal changes in stimulatory and inhibitory receptor expression and intracellular type 2 cytokine expression of ILC2s in the lung using a cecal ligation and puncture mouse sepsis model. We found that IL-13 production by ILC2s, which were predominately composed of the resident natural ILC2 subset rather than the migratory inflammatory ILC2 subset, was reduced in the lungs of sepsis mice on day 1 and gradually restored through day 7. Although the expression levels of ST2 and inducible T-cell costimulator (stimulatory receptors) were high, IL-13 production by ILC2s was reduced while showing high programmed cell death 1 (PD-1) (inhibitory receptor) expression. Furthermore, using IL-33 knockout mice, we have shown that IL-33 regulates the capacity of ILC2s to produce IL-13, possibly through the modulation of ST2 and PD-1 expression and signaling in the septic lung. To the best of our knowledge, this is the first report showing differential costimulatory/inhibitory receptor expression on ILC2s in a septic lung in the context of an IL-33/IL-13 pathway-mediated type 2 immune response in the progression and resolution of inflammation. Our present findings contribute to a better understanding of the underlying immunological mechanism of ILC2s and may fill the critical knowledge gap regarding immune homeostasis in the lung that hampers the development of new therapeutic strategies for sepsis-induced acute lung injury.

KEYWORDS—Acute lung injury, group 2 innate lymphoid cells, IL-13, KLRG1, natural and inflammatory ILC2, PD-1, sepsis, ST2

INTRODUCTION

Unlike classical T or B lymphocytes, the novel types of non-T and non-B lymphocytes discovered in the last decade, termed "innate lymphoid cells" (ILCs), lack adaptive antigen receptors (1). ILC subsets, designated ILC1s, ILC2s, and ILC3s, are identified by the expression of specific transcription factors required for their development and function (2). ILCs are essentially tissue-resident cells and play a pivotal role in regulating the immune network through their role as effector cells of innate immunity (1, 3). They also contribute to the adaptive immune response in the context of host tissue homeostasis, metabolism, inflammation, and tissue repair (1, 3, 4).

Sepsis is a life-threatening organ dysfunction caused by a deregulated immune system response to infection (5). As the lung is among the most affected organs in sepsis (6) we decided to focus on ILC2s, which are the predominant population of tissue-resident ILCs in the lung. ILC2s are characterized by the production of type 2 cytokines such as IL-5 and IL-13. It has been reported that IL-33, which is mainly produced by epithelial cells, can activate ILC2s through the IL-1 receptor family member ST2 (suppression of tumorgenicity 2) receptor (7, 8) and prompt further immune responses. In the lung, these type 2 cytokines are known to contribute to tissue protection from injury (9–11) and immuno-suppression following regulatory T-cell induction (12). However, the functional transition of ILC2s throughout the different time points, early to late phase, during sepsis remains unclear.

The functions of costimulatory/inhibitory molecules, such as inducible T-cell costimulator (ICOS) and programmed cell death 1 (PD-1), are well studied and constitute the crucial regulatory factor as immune-activating (ICOS) (13) and immune-inhibiting (PD-1) (14) receptors not only of T cells,

but also of ILC2s. Furthermore, studying the dynamics of costimulatory/inhibitory molecule expression on T cells during sepsis led to the establishment of new therapeutic strategies (15). Nonetheless, the dynamics underlying ILC2 functions in sepsis remain unknown. Therefore, this study seeks to obtain new insights into the dynamics of costimulatory/inhibitory molecule expression on ILC2 in sepsis, which may help pave the way toward developing new therapeutic strategies. For this purpose, we investigated, in the septic lung, the ILC2 subsets and the temporal changes in the expression levels of ICOS, PD-1, and ST2 on ILC2 and analyzed the relationships between receptor expression, type 2 cytokine expression, and lung patho-histology. In addition, using IL-33 knockout (KO) mice, we have studied the roles of IL-33 in the regulation of IL-13 production and ST2, PD-1, and ICOS expression in the septic lung.

Additionally, we investigated the regulatory roles of the killer cell lectin-like receptor G1 (KLRG1) expressed on ILC2 s. The KLRG1 expressed by NK cells (16) and CD4$^+$ T cells (17) has been shown to mediate inhibitory effects through the recruitment of SHIP-1 and SHP-2. In contrast, the KLRG1 expressed by CD 8$^+$ T cells does not act as an inhibitor (17). Since the regulatory function of KLRG1 expression by ILC2s in the septic lung remains unclear, we have compared KLRG1-negative (KLRG1$^-$) ILC2s and KLRG1-positive (KLRG1$^+$) ILC2s.

MATERIALS AND METHODS

Mice

Female C57BL/6J wild-type (WT) mice were purchased from Japan SLC, Inc (Shizuoka, Japan) and maintained at the Experimental Animal Facility of Mie University. All mice were used between 8 and 12 weeks of age for the experiments. Experimental animal protocols were approved by the Ethics Review Committee for Animal Experimentation of Mie University. *Il33*$^{gfp/gfp}$ mice (Accession No: CDB0631K; www.2.clst.riken.jp/arg/mutant%20mice%20list.html) were kindly provided by Dr S. Nakae (18). Female mice (8–18 weeks) were used for all experiments and followed the guidelines provided by the Institutional Animal Care and Use Committee of RIKEN.

Mouse model of polymicrobial sepsis

Mice were anesthetized with isoflurane (1.5% to 3%) in oxygen, and sepsis was induced using cecal ligation and puncture (CLP) (19). A midline 1-cm incision was made into the peritoneal cavity and the cecum was carefully externalized, of which 50% was ligated. The cecum was perforated using a single through-and-through puncture midway between the ligation and the tip of the cecum. A 21-gauge needle was used in a mesenteric-to-antimesenteric direction to avoid puncturing blood vessels. A small amount of feces was gently squeezed out of the perforation site to ensure the patency of punctures. The cecum was then returned to the peritoneal cavity, and the wound was sutured in two layers (muscular and dermal) with 6-0 nylon. Finally, mice were subcutaneously injected with saline (0.9% w/v, 1 mL) for fluid resuscitation immediately after surgery. As a control group, mice in the sham group underwent laparotomy without ligation and puncture, but the cecum was externalized. The healthy group that had not undergone any surgery was also used for control purposes. Antibiotics were not administered to experimental or sham mice after surgery.

Histological analysis of lung injury

Lung injury was induced using CLP. Lung samples were fixed in 10% formalin-neutral buffer solution overnight and transported to the Central Institute for Experimental Animals (Kanagawa, Japan) for histological analysis. Samples were dehydrated, embedded in paraffin, and cut into 3-μm-thick sections, which were stained with hematoxylin and eosin. Histological assessment of lung injury was performed according to the scoring system of the American Thoracic Society (20). Briefly, 20 random fields (400 × magnification) against a lung were independently scored by two researchers. Values = 0, 1, or 2 represent the severity according to the findings as follows: neutrophils in the alveolar space, neutrophils in the interstitial space, hyaline membranes, proteinaceous debris filling the airspaces, and alveolar septal thickening. A standardized histological injury score was calculated as follows: score = [20 × (i) + 14 × (ii) + 7 × (iii) + 7 × (iv) + 2 × (v)]/(number of fields × 100). The total score was a continuous value between 0 (normal) and 1 (most severe injury). The score was the average of the values independently calculated by two researchers.

Isolation of leukocytes from the lung

Lung tissues were minced into small pieces and twice incubated with 1 mg/mL collagenase (Fujifilm Wako Pure Chemical Corporation, Osaka, Japan) for 45 min at 37°C. Tissue pieces were removed by an iron mesh and the supernatant, including the leukocytes, was centrifuged. Seventy percent Percoll was layered onto the cells suspended with 40% Percoll (GE Healthcare, Stockholm, Sweden) and centrifuged at 2,000 rpm at 25°C for 20 min. The middle-layer after the Percoll gradient was treated with ACK (Ammonium-Chloride -Potassium) Lysing Buffer (150 mM NH$_4$Cl, 10 mM KHCO$_3$, 0.1 mM EDTA) to remove the red blood cells.

Flow cytometry

Cell suspensions were incubated with a combination of monoclonal fluorescently conjugated antibodies as follows: CD45.2-PerCP (104, BioLegend), ST2- PE/Cy7 (DIH4, BioLegend), PD-L1- PE/Cy7 (10F.9G2, BioLegend), CD127- PE/Cy7 (A7R34, BioLegend), CD90.2-APC/Fire 750 (30-H12, BioLegend), ICOS-APC (C398.4A, BioLegend), PD-1-APC (29F.1A12, BioLegend), IL-5-PE (TRFK5, Thermo Fisher Scientific), IL-13-PE (eBio13A, Thermo Fisher Scientific), Rat IgG 1 kappa isotype control-PE (eBRG1, Thermo Fisher Scientific), KLRG1-PE (2F1, BD Biosciences), ST2-BV421 (U29–93, BD Biosciences), KLRG1-BV421 (2F1, BD Biosciences). The lineage cocktail for the FITC-conjugated antibodies was as follows: CD3ε (145-2C11, BioLegend), CD4 (RM4-4, BioLegend), CD19 (1D3/CD19, BioLegend), CD11b (M1/70, BioLegend), CD11c (N418, BioLegend), TCRβ (H57-597, BioLegend), TCR γ/δ (GL3, BioLegend), Gr1 (RB6-8C5, BD Biosciences), NK1.1 (PK136, BioLegend), FcεRI (MAR-1, BioLegend), and Ter119 (TER-119, BD Biosciences). ILC2 s were identified using flow cytometry as Lin$^-$ CD45.2$^+$CD90.2$^+$ST2$^+$. The absolute number of cells was calculated as follows: percentage of ILC2 s × absolute lymphocyte count.

To analyze intracellular protein expression, cells were incubated with phorbol 12-myristate 13-acetate (50 ng/mL), ionomycin (500 ng/mL) in the presence of GolgiStop (BD Biosciences) for 4 h. Cells were analyzed on a CantoII flow cytometer (BD Biosciences). Intracellular staining was performed using an Intracellular Fixation and Permeabilization Buffer Set (Thermo Fisher Scientific, Waltham, Mass). Positive signals were identified by comparing staining with isotype-matched control antibodies or a Fluorescence minus one control. Fc block (BD Biosciences) was used to prevent nonspecific antibody binding. Cell viability was determined using a Zombie Aqua Fixable Viability Kit (BioLegend, San Diego, Calif). Data were analyzed using FlowJo software.

RNA isolation and real-time quantitative PCR

Total RNA from lung tissue was isolated using Trizol reagent (Thermo Fisher Scientific) according to the manufacturer's instructions. Reverse transcription (RT) was performed using a PrimeScript RT reagent kit (Takara Bio). RNA purity (A$_{260}$/A$_{280}$ ratio ≧ 1.8) and concentrations were measured using Nanodrop. Quantitative real-time PCR was performed using SYBR Green (Thermo Fisher Scientific) with a StepOne system (Thermo Fisher Scientific) for measuring IL-33 and PD-L1 mRNA expressions. *Actb* mRNA served as an endogenous control to normalize mRNA levels (21) using the comparative Ct method. Primer sequences were as follows: *Actb*, forward 5′- CATCG-TACTCCTGCTTGCTG -3′ and reverse 5′- AGCGCAAGTACTCTGTGTGG -3′; IL-33, forward 5′- TGAGACTCCGTTCTGGCCTC -3′ and reverse 5′- CTCTTCATGCTTGGTACCCGAT -3′; PD-L1, forward 5′- GACCAGCTTTT-GAAGGGAAATG -3′and reverse 5′- CTGGTTGATTTTGCGGTATGG -3′.

TaqMan assays were used for the detection of *Il25* and *Il33* mRNA expression. TaqMan probes purchased from the Thermo Fisher Scientific were as follows: *Il25* (Mm00499822), *IL33* (Mm00505403), and *Gapdh* (Mm99999915). Data were normalized with *Gapdh* mRNA.

Statistical analysis

Statistical analysis was performed using Prism 8 (GraphPad Software), and $P < 0.05$ indicated a significant difference. The values of the mean and standard error of the mean are presented.

RESULTS

CLP-induced mortality

Sepsis was induced in mice subjected to CLP. Kaplan–Meier analysis revealed a significantly shorter time-to-death among the CLP group of C57BL/6J WT female mice compared with that of the sham group. Seven days after surgery, all mice in the sham group were alive compared with 32.4% ($P < 0.0012$) of the mice that underwent CLP (Fig. 1A). The weights of CLP mice decreased from their baseline values (Fig. 1B). The rate of bodyweight loss of the CLP mice was greater compared with that of the sham mice on days 3 and 7, but lower on day 1 (Fig. 1B), although the CLP mice appeared weaker. The average bodyweight loss was greatest on day 3, recovering to normal values during days 3 through 7 (Fig. 1C).

Tissue injury and IL-33 expression in the lung

Histological examination was performed to investigate the lung injury induced by sepsis. Lung tissue sections were stained with hematoxylin and eosin (Fig. 2A). Histological assessment of lung injury was carried out according to the scoring system of the American Thoracic Society (20). Specifically, 20 random fields (×400magnification) were independently scored by two researchers. Each of the five histological findings was graded in a three-tiered manner as described above. Block arrows indicate neutrophils in the lung after CLP. Lung injury scores of the CLP mice significantly increased after 6 h and on days 1, 3, and 7 after surgery compared with those of healthy mice (Fig. 2B). The main influence on scores was early infiltration of the lungs by neutrophils (Fig. 2A), which was consistent with inflammatory changes in the lungs. We were unable to find any hyaline membranes in the pathological tissue, as one previous study reported (20). These data support the occurrence of sepsis-induced inflammation in the lung.

We next determined lung levels of the mRNA encoding IL-33, which activates ILC2s through ST2 (7). Consistent with the results of other studies, the levels of Il33 mRNA expression peaked after 6 h, returning to baseline after 24 h (9, 10). They subsequently peaked again on day 3 (Fig. 2C). These bimodal peaks reflected the values of the lung injury score (Fig. 2, B and C). Our results are consistent with the production of IL-33 in the lung by epithelial cells in epithelial barrier tissues (22).

Temporal changes in cytokine expression by ILC2s in the septic lung

Flow cytometry identified Lin⁻CD45.2⁺CD90.2⁺ST2⁺ cells as ILC2s on days 1, 3, and 7 after laparotomy or CLP (Fig. S1A, http://links.lww.com/SHK/B120). Furthermore, we determined that these cells expressed the ILC2 markers ICOS and CD127 (1), thus reconfirming them as ILC2s (Fig. S1B, http://links.lww.com/SHK/B120). The absolute number of ILC2s in the lungs 1 day after surgery was significantly higher in CLP mice than in sham-operated mice, while there were no significant differences between the CLP mice and sham mice on days 3 and 7 after surgery (Fig. 3A). Representative flow cytometry histograms of Lin⁻CD45.2⁺CD90.2⁺ST2⁺ILC2s are shown in Figure 3B.

Next, we investigated the expression of IL-5 and IL-13 by ILC2s (Fig. 3C, S2, http://links.lww.com/SHK/B121) in the septic mouse lung. IL-13 levels were significantly different between the CLP and sham mice, in contrast to those of IL-5, which did not significantly differ. IL-13 levels were lower in CLP mice compared with those of sham mice on day 1, but higher on day 7.

Temporal changes in the expression of cell-surface markers and immune modulators by ILC2s in the septic lung

We next analyzed temporal changes in ST2 expression by ILC2s to evaluate the signaling of the IL-33/ST2 pathway in the septic lung. ST expression on lung ILC2s was increased on days 1 and 7, but decreased on day 3 in CLP mice (Fig. 4A), which failed to synchronize to the lung IL-33 mRNA expression level that peaked on day 3 (Fig. 2C). This result suggests that the strength of IL-33/ST2 signaling on day 3 was weakened, thereby explaining why IL-5 and IL-13 production did not increase on day 3. However, changes in the production of IL-5 and IL-13 cannot simply be explained by differences in IL-33 signaling and ST2 expression. For example, the levels of secreted IL-13 in the lung decreased on day 1, while those of ST2 and Il-33 did not (Figs. 2C, 3C, 4A). These results suggest that the ability of ILC2s to produce IL-5 and IL-13 was not regulated solely by the IL-33/ST2 pathway in the septic lung.

To study pathways other than IL-33/ST-2 that regulate IL-5 and IL-13 production in lung ILC2s, the levels of immune-activating (ICOS) and immune-inhibitory (PD-1) surface proteins were analyzed using flow cytometry. ICOS is a costimulatory receptor that is required for T-cell activation and function (23). In addition, ICOS:ICOSL interactions on ILC2s promote the production of type 2 cytokines and cell survival through STAT5 signaling (13). We found that the levels of ICOS increased in CLP mice on days 1 and 7 (Fig. 4B). This result is similar to that for ST2 expression, except that the levels of ICOS did not decrease by day 3 compared with those of sham mice.

PD-1 inhibits both T cells and NK cells (24, 25) and functions similarly in ILC2s (14). Although the levels of PD-1 expressed by ILC2s peaked on day 3 after CLP, they remained significantly higher than those of sham mice throughout the experiment (Fig. 4C). This result suggests that the PD-1/PD-L1 pathway functions as an additional mechanism regulating the ability of ILC2s to produce IL-5 and IL-13, possibly counter-balancing the IL-33/ST2 pathway in the septic lung.

ILC2 subset analysis in the septic lung

Two distinct subsets of ILC-2, natural ILC2 (nILC2) and inflammatory ILC2 (iILC2), have been identified. nILC2s, which respond to IL-33, constitute the major subset of tissue-resident ILC2s, whereas iILC2s, which respond to IL-25, are thought to migrate between organs in response to external stimulations (26). As iILC2s have been shown to migrate to the lung from the intestine in response to helminth infection or exogenous IL-25 administration (27), it would be extremely interesting to determine whether iILC2s accumulate in the inflamed lung due to polybacterial peritonitis in the CLP sepsis model. Representative flow cytometry histograms of iILC2s were observed (Fig. 5A), showing that iILC2s not expressing
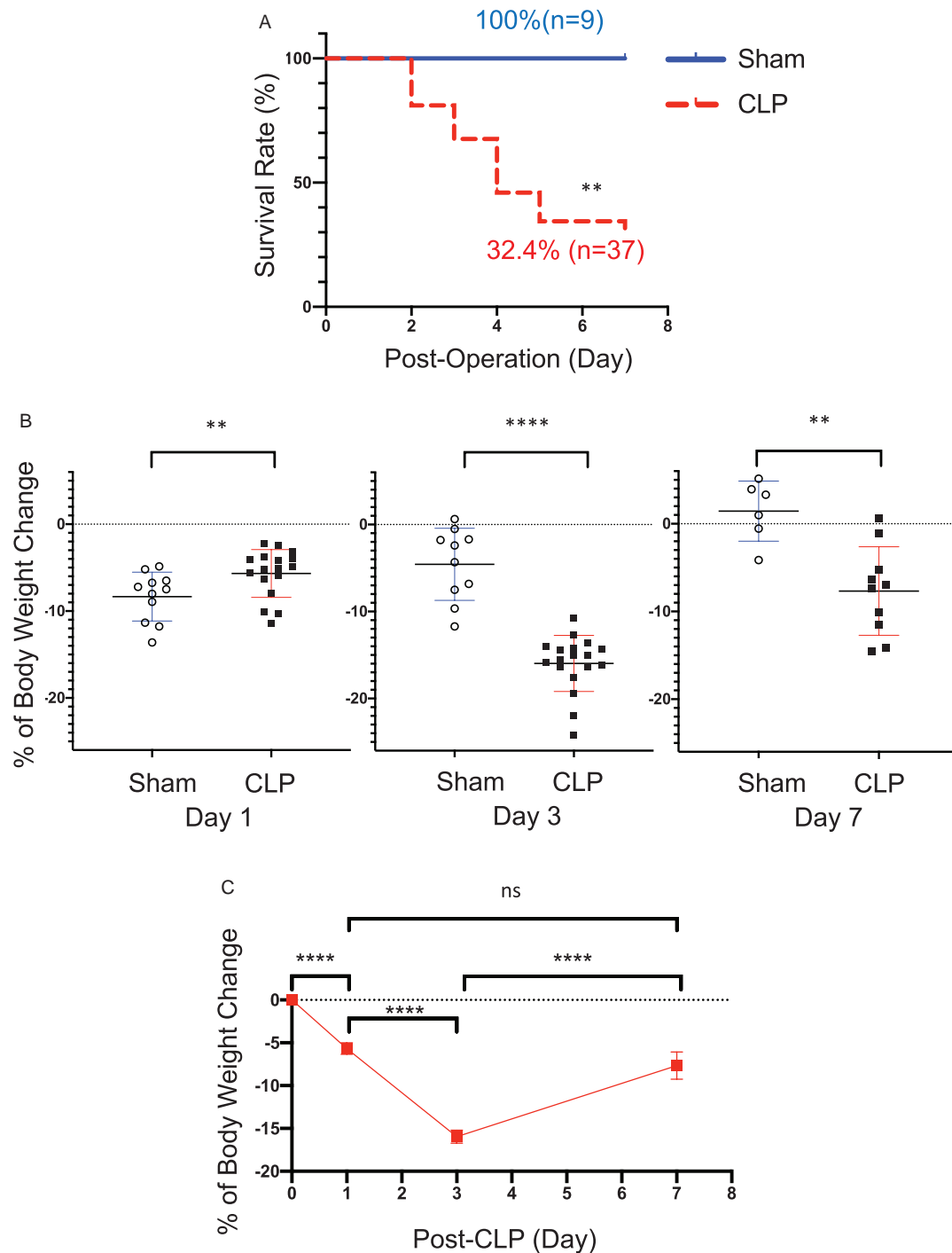
FIG. 1. **CLP-induced mortality.** (A) Survival curve of mice including both sham and CLP groups (CLP: n = 37, sham: n = 9). Survival rates were analyzed using the log-rank (Mantel-Cox) test. (B) Comparison of body weight changes in sham and CLP mice. The data from sham (n = 6–11 per group) and CLP (n = 10–18 per group) mice were evaluated using the Mann–Whitney test. (C) Comparison of body weight changes of CLP mice during the experiment period. The data from CLP (n = 10–18 per group) mice were evaluated using a Kruskal–Wallis test; which was followed by a Dunn multiple comparison test of multiple groups. Data represent the mean ± SEM. ns indicates not significant; CLP, cecal ligation and puncture. **P < 0.01, ****P < 0.0001.

ST2 were identified as Lin⁻CD45.2⁺CD90.2⁺ST2⁻KLR-ST2⁻KLRG1^high (Fig. S1A, http://links.lww.com/SHK/B120) (28). We did not observe any significant increase in the number of iILC2 s in the septic lungs (Fig. 5B), thereby confirming that nILC2 s represent the major ILC2 subset in septic lungs (Fig. 5C). We have shown in lung tissues that the expression of IL-33, which activates nILC2 s, was readily detectable throughout the time course of septic lung progression and was upregulated on day 3. By contrast, the expression of IL-25, which activates iILC2 s, was barely detectable in the septic lung (Fig. 5D), thereby explaining the lack of iILC2 accumulation therein.
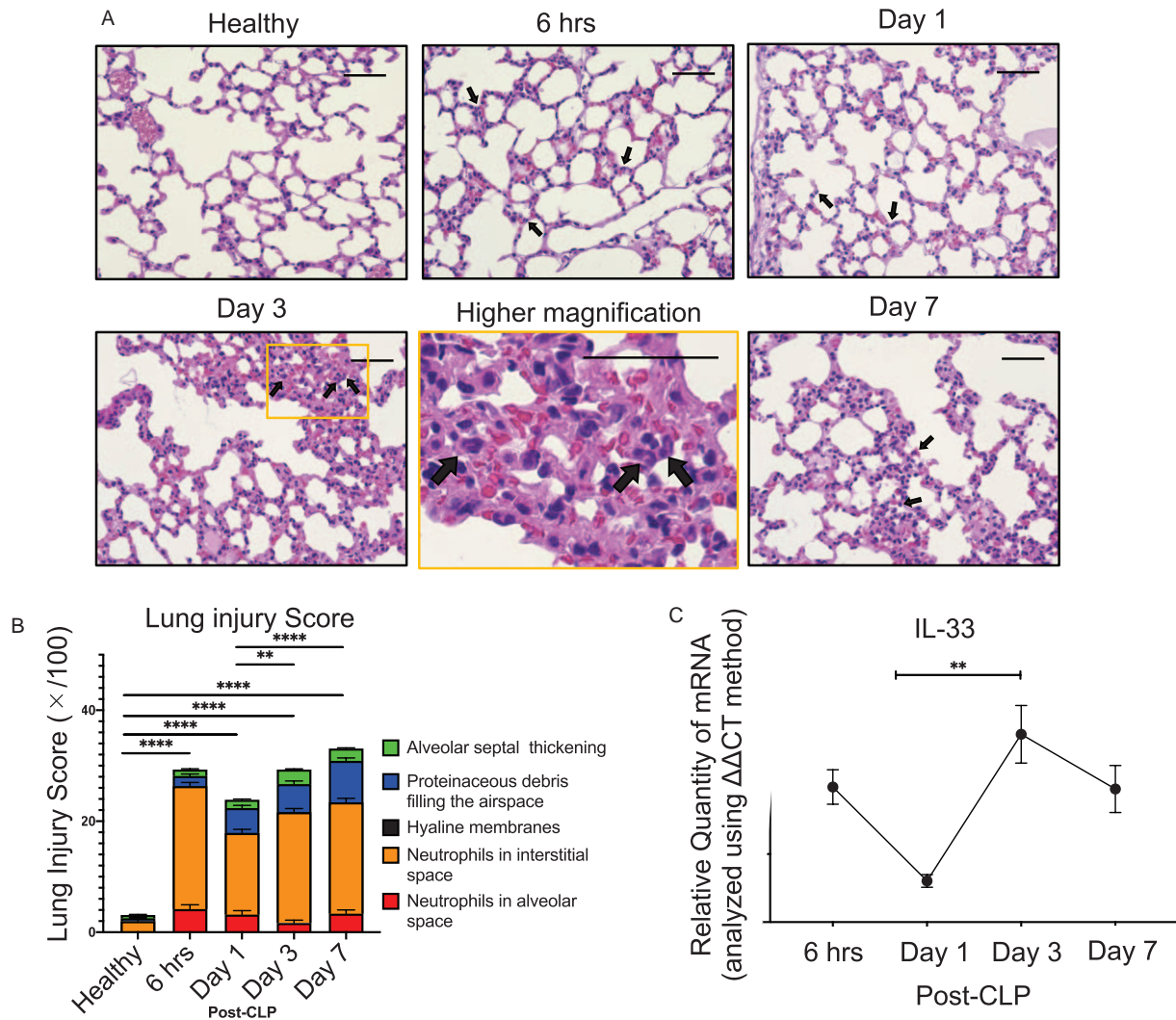
FIG. 2.   **Evaluation of lung injury and IL-33 expression in the lung.** (A) Histological images of mice lungs from 0 h, 6 h, 1 day, 3 days, and 7 days after CLP. Healthy mice were used for control purposes. Sections were stained with hematoxylin and eosin (H&E) and are shown at ×400 original magnification. Block arrows indicate neutrophils in the lung after CLP. Images are representative of twice carried-out independent experiments. Scale bars; 50 μm. (B) Injury scores of mice lungs from the CLP group and the healthy group without any surgery (n = 3 females from each group). The sums of the histology scores of the five parameters were calculated; 20 random fields (×400 magnification) against the lung were independently scored by two researchers. (C) The mRNA level of IL-33 in the lung was evaluated (n = 4 per each group). The Kruskal−Wallis test was followed by a Dunn multiple comparison test to compare multiple groups. Data represent the mean ± SEM. $^{**}P < 0.01$, $^{****}P < 0.0001$. CLP indicates cecal ligation and puncture.

Roles of IL-33 on nILC2 regulation in the septic lung

To further investigate the roles of IL-33, a cytokine that activates nILC2 s, in the septic lung, we utilized IL-33-deficient mice (18). The induction of sepsis by CLP in IL-33 KO mice resulted in progressive bodyweight loss. Compared with WT mice subjected to CLP, IL-33 KO mice exhibited significantly more severe bodyweight loss at day 7 (Fig. 6A). Before CLP, IL-33 KO mice showed reduced numbers of lung ILC2 s compared with WT (IL-33 KO, 5,541 ± 3,615, n = 3; WT 30,180 ± 3,972, n = 5). The numbers of nILC2 s in the lung on days 1 and 7 were significantly lower in septic IL-33 KO mice compared with septic WT mice (Fig. 6B). Only very minor iILC2 accumulations were observed in the lungs of either WT or IL-33 KO mice (Fig. 5B and not shown). Furthermore, the number of IL-13-producing nILC2 in the lung was also significantly reduced in septic IL-33 KO mice on day 7, compared with septic WT mice

(Fig. 6C). In addition, the expression on lung nILC2 s of ST2 and PD-1, but not ICOS, was significantly reduced in septic IL-33 KO mice on days 1 and 7, compared with septic WT mice (Fig. 6, D–F).

Phenotypic analysis of KLRG1$^+$ and KLRG1$^-$ ILC2 s in the septic lung

To investigate the biological function of KLRG1 expressed by ILC2 s, we compared the expression of IL-5 and IL-13 by KLRG1$^+$ and KLRG1$^-$ ILC2 s (Fig S3, http://links.lww.com/SHK/B122), which populate the septic lungs of female mice (29). The IL-5 levels produced by KLRG1$^+$ ILC2 s in the lung were significantly higher compared with those of KLRG1$^-$ ILC2 s on days 3 and 7 after CLP, as were those of IL-13 on day 1 (Fig. 7). Furthermore, KLRG1$^+$ ILC2 s produced higher levels of IL-5 and IL-13 compared with those of KLRG1$^-$ ILC2 s throughout the experiment, although some differences
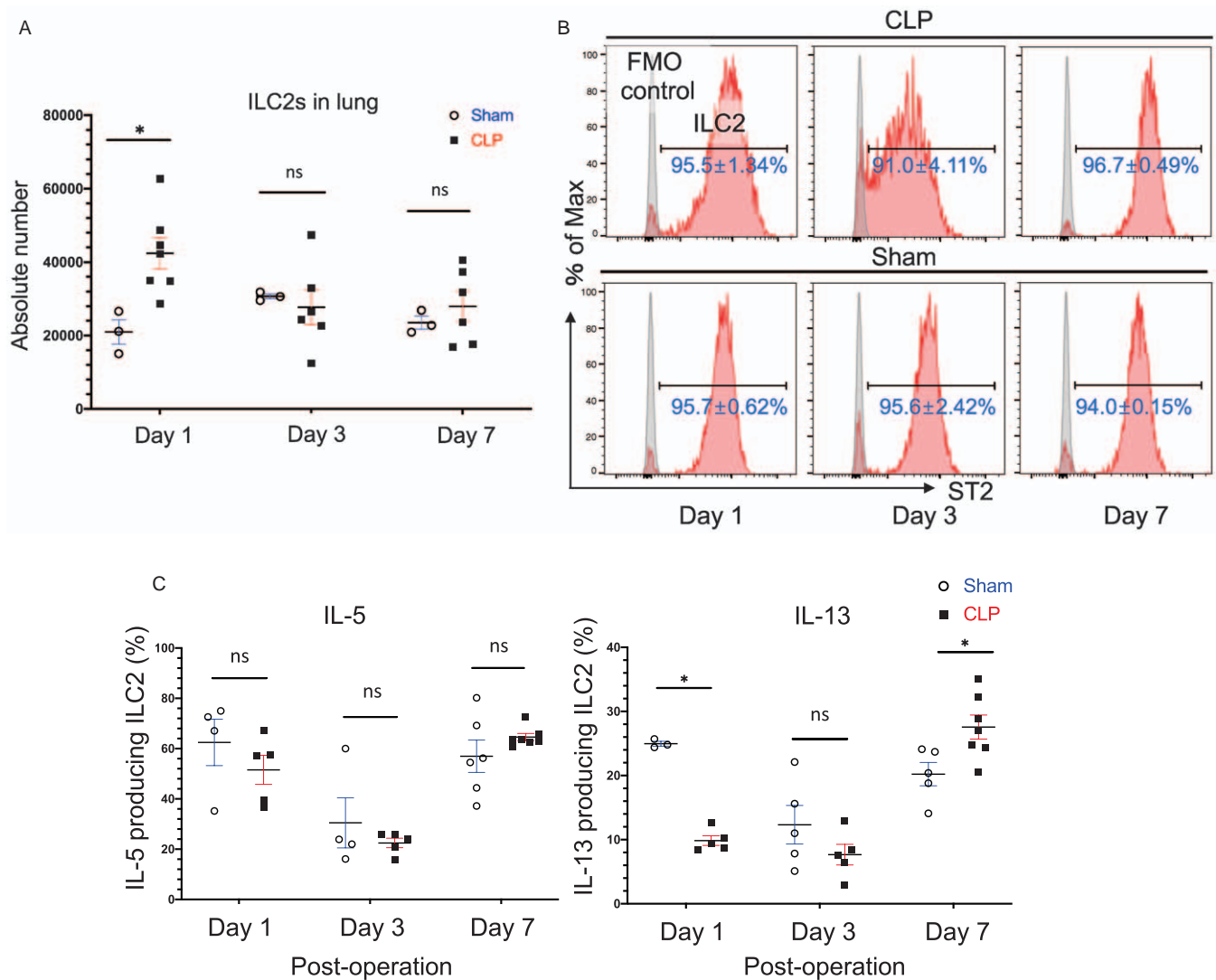
FIG. 3.   **Temporal changes in the expression of cytokines by ILC2 s in the septic lung.** (A) Absolute numbers and (B) representative flow cytometry histograms of lung ILC2 s in WT female mice after laparotomy and CLP. (C) Percentage of IL-5- and IL-13-producing ILC2 s. Cells were stimulated with PMA (50 ng/mL) and ionomycin (500 ng/mL) in the presence of GolgiStop™ (BD Biosciences). Cells were incubated for 4 h before the analysis of intracellular cytokine detection. The data were compiled from two or three independent experiments. The data from sham mice (n = 3−5 females per group) that underwent laparotomy and CLP (n = 5−7 females per group) mice were evaluated using the Mann−Whitney test. Data represent the mean ± SEM. ns indicates not significant; ILC2 s, group 2 innate lymphoid cells; CLP, cecal ligation and puncture; PMA, phorbol 12-myristate 13-acetate; WT, wild-type. $^{*}P < 0.05$.

were not statistically significant (Fig. 7). These results indicate that KLRG1 may not act as an inhibitory receptor in the septic lung. To assess the status of KLRG1^{+} and KLRG1^{-} ILC2 s in the septic lung, surface marker levels and absolute cell numbers were analyzed using flow cytometry. The levels of PD-1 expressed by KLRG1^{+} ILC2 s were significantly higher compared with those of KLRG1^{-} ILC2 s on days 1 and 7 after CLP (Fig. 8). In contrast, the levels of ST2 and ICOS did not significantly differ between the two groups (Fig. 8).

DISCUSSION

One of the main goals of our study was to reveal the dynamics of costimulatory/inhibitory receptor expression on ILC2 in sepsis-induced lung inflammation, and to analyze the relationships between receptor expression, cytokine producibility, and lung patho-histologies. Our results have revealed time-dependent changes in costimulatory/inhibitory receptor and cytokine expression on ILC2 s in the septic lung. These results have uncovered the following information. First, sepsis induced deregulation of IL-13 production in lung ILC2 s, the majority of which are composed of IL-33-responsive nILC2 s, but not IL-25-responsive iILCs. Second, aberrant regulation of IL-13 expression occurred in tandem with high PD-1 expression on ILC2 s. Third, the experiments using IL-33 KO mice have shown that IL-33 contributes to the regulation of ILC2 to produce IL-13 and express ST2 and PD-1 in the septic lung. Finally, KLRG1, which acts as an inhibitory receptor in T and NK cells, may be involved in ILC2 activation.

IL-13 production by ILC2 s in the lung was initially inhibited by sepsis on day 1, and gradually increased by day 7 (Fig. 3C). Although the lung injury scores remained significantly higher in CLP mice than in healthy controls during days 1 through 7
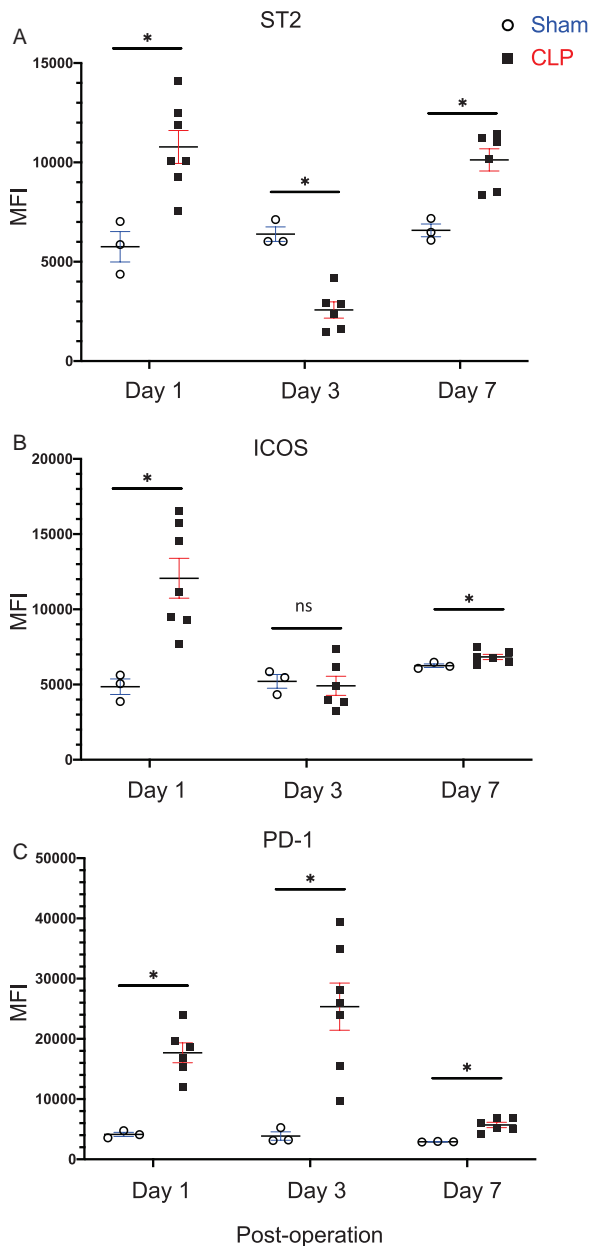
FIG. 4.   **Temporal changes in the expression of cell-surface markers and immune modulators by ILC2 s in the septic lung.** Mean fluorescence intensity (MFI) of (A) ST2, (B) ICOS, and (C) PD-1 expressed on ILC2 s. The data from sham mice (n = 3 females per group) and CLP (n = 6−7 females per group) mice were evaluated using the Mann–Whitney test. ns indicates not significant; ILC2 s, group 2 innate lymphoid cells; PD-1, programmed cell death 1; ICOS, inducible T-cell costimulator. *P < 0.05.

ILC2 s might play an important role in linking systemic inflammation to lung inflammation in sepsis. Thus, deregulation of IL-13 production by ILC2 s may be associated with the pathogenesis of sepsis-induced lung inflammation. On the other hand, IL-5 levels were not significantly different between CLP and sham mice during the experimental period (Fig. 3C). It appears that IL-13 production was more readily influenced than that of IL-5 in the septic lung.

IL-13 has been shown to exert a protective role in sepsis. Antibody-mediated neutralization of IL-13 in a CLP sepsis mouse model has been shown to worsen mortality and lung injury, which are associated with increased neutrophil-activating chemokine and proinflammatory cytokine levels in the lung (31). These findings support the concept that IL-13 plays a crucial role in preventing sepsis-induced lung injury by suppressing inflammation and/or promoting resolution of inflammation. Our result showed that the IL-13 levels generated by ILC2 s in the septic lung were significantly lower on day 1 (Fig. 3C), thereby suggesting that deregulation of ILC2 s in the septic lung may contribute to the pathogenesis of lung injury. ILC2 s in the lung contribute to polarizing alveolar macrophage to the M2 phenotype by secretion of IL-13 in vitro (32). A recent study demonstrated that M2 macrophages adoptively transferred into acute lung injury (ALI) mice significantly reduced lung inflammation and injury (33), indicating that a rapid shifting to M2 macrophages may limit lung inflammation and injury. The restoration of IL-13 production by ILC2 s may protect against inflammation by inducing the M2 polarization of macrophages.

To study how sepsis reduced IL-13 production in ILC2 on day 1, we investigated the balance between the stimulatory receptors ST2 and ICOS and the inhibitory receptor PD-1 on ILC2 s. In sepsis, the levels of PD-1 and PD-L1 expressed by T cells and monocytes, respectively, are upregulated (34). Here we show that the levels of PD-1 expressed by ILC2 s were also markedly higher in CLP mice (Fig. 4C), particularly on days 1 and 3. This may explain how the expression level of IL-13 was negatively regulated by PD-1/PD-L1 signaling on day 1, despite the fact that ILC2 s express good levels of the stimulatory receptors ST2 and ICOS (Figs. 3C, 4A–C).

Blocking PD-1/PD-L1 signaling has been shown to improve the outcome of CLP-induced sepsis in mice (35, 36). The therapeutic effects have been thought to be mediated primarily by ameliorating T-cell exhaustion. Our results suggest an alternative/additional explanation whereby blocking PD-1/PD-L1 signaling might also act on ILC2, thereby exerting beneficial effects to relieve the suppression of IL-13 production on ILC2 s. These findings may help to explain the novel mechanisms of the therapeutic efficacy achieved by blocking PD-1/PD-L1 signaling on ILC2 s in sepsis-induced lung injury. Therefore, our findings may contribute to the cellular basis and formulation of new therapeutic targets for sepsis-induced acute lung injury.

The level of IL-13 expressed by ILC2 s in the septic lung on day 3 was not significantly lower than that of the sham mice, although the PD-1 levels remained high (Figs. 3C, 4C). The PD-L1 levels in the lung tissues of CLP mice were significantly lower on day 3 compared with those on day 1 (Fig. S4,

(Fig. 2B), bodyweight had recovered during days 3 through 7 after CLP (Fig. 1, B and C). Furthermore, IL-33 mRNAs in the lung tissues, which are thought be upregulated in the injured pulmonary epithelial cells (30), also trended to decreased levels on day 7 (Fig. 2C), thereby suggesting an ongoing process of inflammatory resolution by day 7. Interestingly, these results indicated that ILC2s mediated the maintenance of tissue immune homeostasis at the molecular level (i.e., restoration of IL-13 expression) (1), which might precede the resolution of pulmonary inflammation at the histological level.
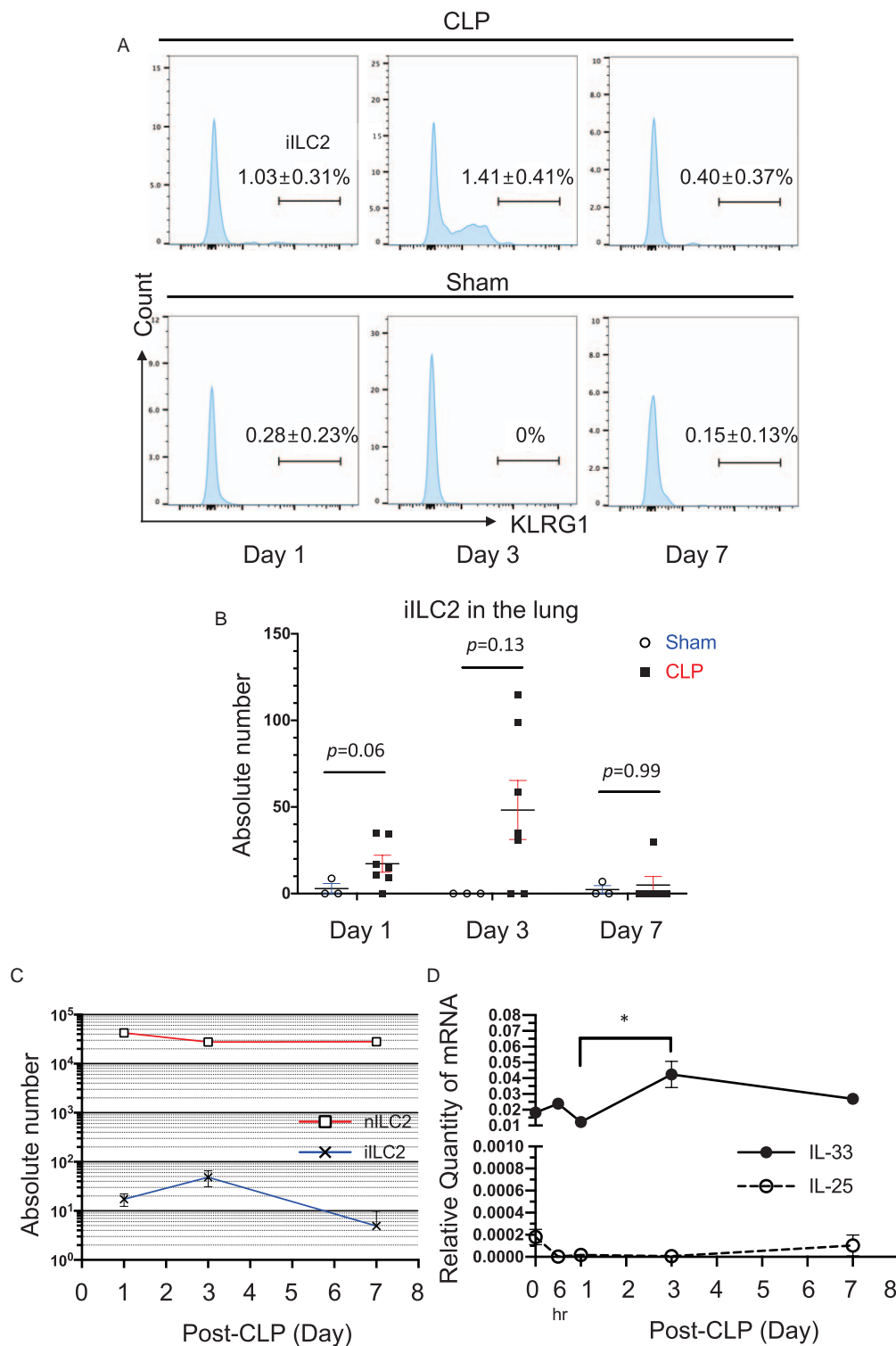
Fig. 5. **ILC2 subset analysis in the septic lung.** (A) Representative flow cytometry histograms and (B) absolute numbers of iILC2 (Lin⁻ CD45.2⁺CD90.2⁺ST2⁻KLRG1^high) in WT female mice after laparotomy and CLP. The data were analyzed using the Mann–Whitney test. (C) Comparison of natural ILC2 s and inflammatory ILC2. (D) Comparison of the mRNA level of IL-25 and IL-33 (n = 3–4 per each group). Dots at 0 h denote the control data of untreated mice. The Kruskal–Wallis test followed by a Dunn multiple comparison test was used to compare multiple groups. Data represent the mean ± SEM. *$P < 0.05$. ILC2 s indicates group 2 innate lymphoid cells; WT, wild-type; KLRG1, killer cell lectin-like receptor G1.

http://links.lww.com/SHK/B123), suggesting that PD-1/PD-L1 signaling by ILC2 s was weaker on day 3 than on day 1. This result may explain why the levels of IL-13 produced by ILC2 s in the septic lung were not lower on day 3 (Fig. 3C), although the PD-1 levels were still high (Fig. 4C).

How signaling through ST2 and PD-1 on ILC2 s is deregulated in sepsis remains to be elucidated. In both T cells (37) and ILC2 (38, 39) it has been shown that IL-33/ ST2 signaling induces the recruitment of myeloid differentiation primary response protein 88 to the cytoplasmic region
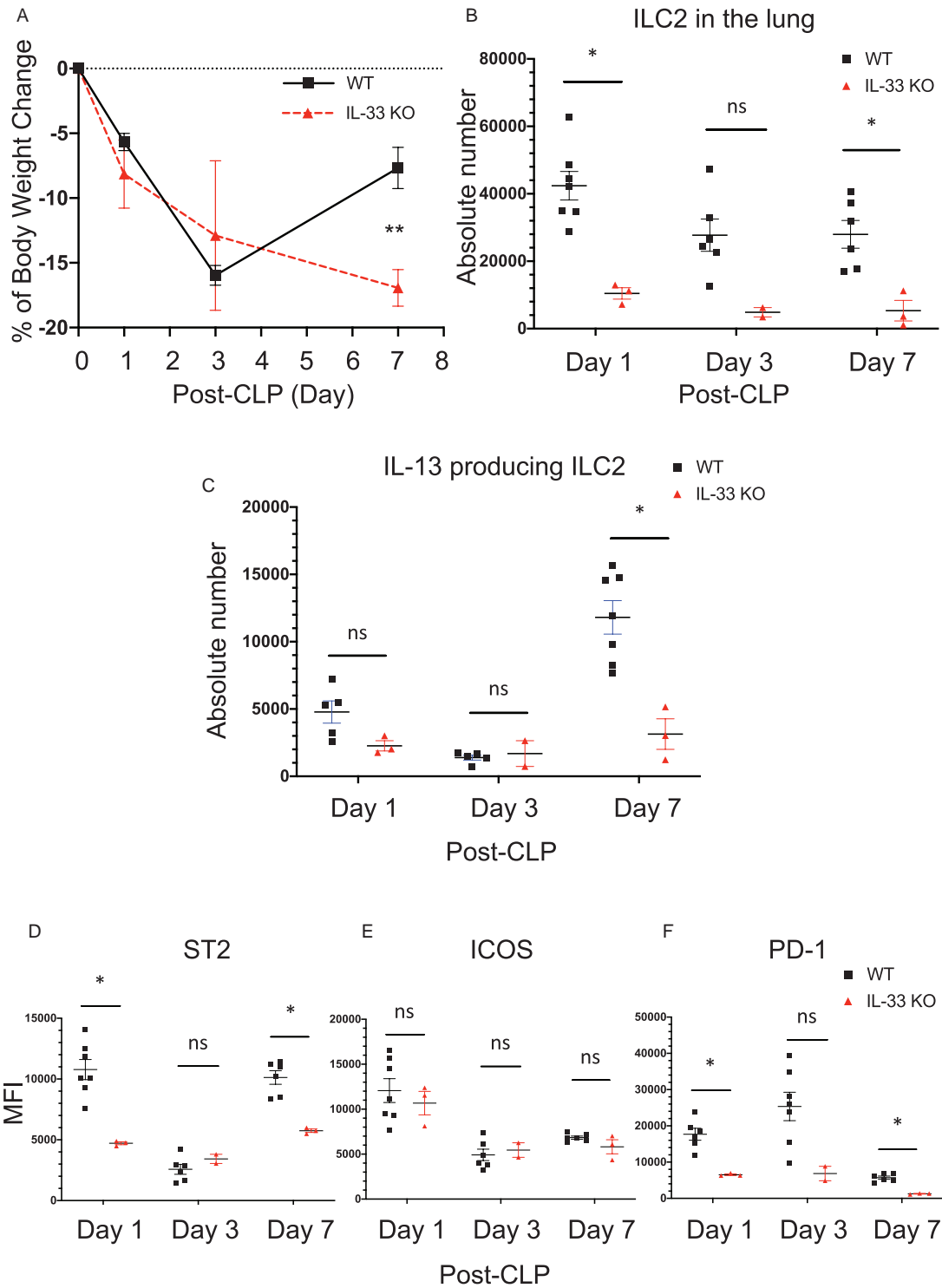
Fig. 6.   **Roles of IL-33 on nILC2 regulation in the septic lung.** (A) Comparison of body weight changes in WT and IL-33 KO female mice after CLP. (B) Absolute numbers of lung ILC2 s in WT and IL-33 KO mice after CLP. (C) Absolute numbers of IL-13-producing ILC2 s in WT and IL-33 KO mice. (D) ST2, (E) ICOS, and (F) PD-1 expressions on ILC2 s after CLP. The data from WT mice (n = 6−7 females per group) and IL-33 KO mice (n = 2−3 females per group) were analyzed using the Mann−Whitney test. ns indicates not significant; ILC2 s, group 2 innate lymphoid cells; WT, wild-type; ICOS, inducible T-cell costimulator ; PD-1, programmed cell death 1; KO, knockout. $^*P < 0.05$, $^{**}P < 0.01$. Data represent the mean ± SEM.

of ST2. This leads to the activation of NF-kB and AP-1 pathways, thereby leading to the upregulation of IL-13 expression. PD-1 signaling in T cells inhibits both CD28 and TCR-mediated activation by recruiting SHP-2, thereby dephosphorylating their downstream signaling molecules within the PI3K/AKT and MAPK/ERK signaling pathways (40). By contrast, PD-1 suppresses ILC2 function through a different mechanism, i.e., via the inhibition of STAT5 phosphorylation (14). Interestingly, the proportion and intensity of PD-1 expression on ILC2 s were increased by IL-33
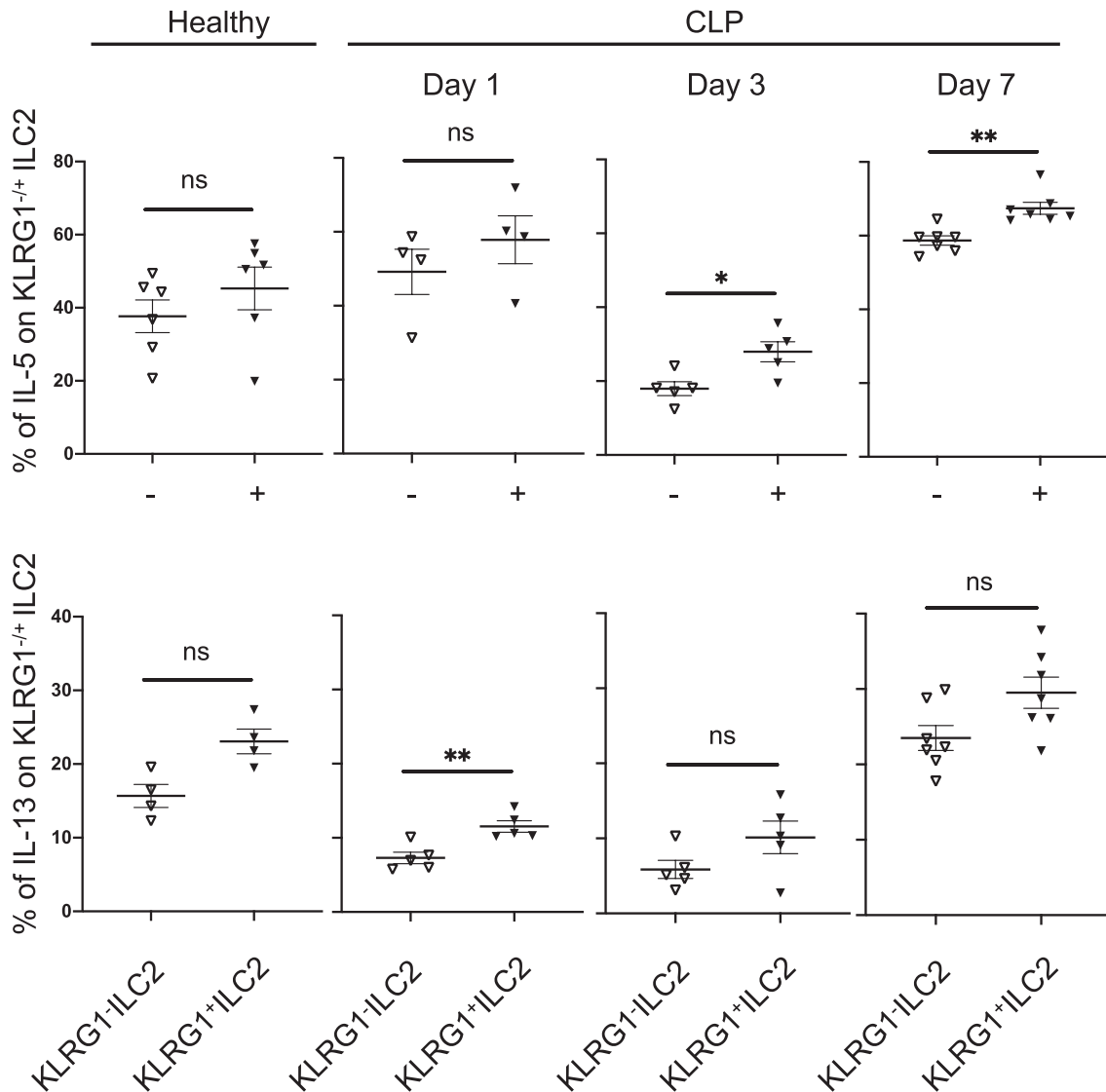
Fɪɢ. 7.   **Cytokine expression by KLRG1$^+$ and KLRG1$^-$ ILC2 s in the lung during sepsis.** Percentage of IL-5- and IL-13-producing KLRG1-negative and -positive ILC2 s in the lungs of healthy and CLP mice. The data were evaluated using the Mann−Whitney test. Data represent the mean ± SEM. ns indicates not significant; KLRG1, killer cell lectin-like receptor G1; ILC2 s, group 2 innate lymphoid cell; CLP, cecal ligation and puncture. $^*P < 0.05$, $^{**}P < 0.01$.

stimulation (41), potentially constituting a negative feedback mechanism.

In the interstitial space of the lung, ILC2 s are located in collagen-rich regions near the confluence of medium-sized blood vessels and the airway (42). Macrophages are also present in the interstitial space of the lung (43). IL-33, which stimulates lung ILC2 s and promotes IL-5 and IL-13 production (7), is predominantly expressed by damaged lung epithelial cells (22). Remarkably, IL-33 is cleaved by apoptosis-associated caspases such as caspase-3 and -7, but not by inflammation-associated caspases such as caspase-1, -4, and -5 (44). PD-L1 is expressed by endothelial cells, lung epithelial cells, fibroblasts, and macrophages (45). The expression levels of PD-L1 are induced by proinflammatory cytokines, including TNF-α and IFNγ, and IL-10 (45). We would like to propose that the balance between IL-33/ST2 and PD-L1/PD-1 sigaling in the lung interstitial microenvironment might be responsible for the

regulation of IL-13 expression in ILC2 (Fig. 9). Even though our concept requires further study, we think that our research is notable in that we investigated PD-1 expression levels on ILC2 s and examined the possibility that PD-1 mediates the inhibition of ILC2-derived IL-13 production, driving this newly described therapeutic effect by blocking PD-1/PD-L1 signaling in the sepic lung.

We have performed additional CLP experiments using KO mice that lack expression of IL-33, the critical activator for nILC2 s that induces/maintains cellular proliferation (46) and expression of ST2 (46) and PD-1 (41). The sepsis-induced increase of ILC2 s in the lung observed in WT mice on day 1 was absent in IL-33 KO mice. In addition, the number of ILC2 s in IL-33 KO septic lungs remained lower compared with WT septic lungs (Fig. 6B). In the ILC2 s of IL-33 KO septic lungs, the surface expression of ST2 (positive regulator of IL-13 production) and PD-1 (negative regulator of IL-13 production)
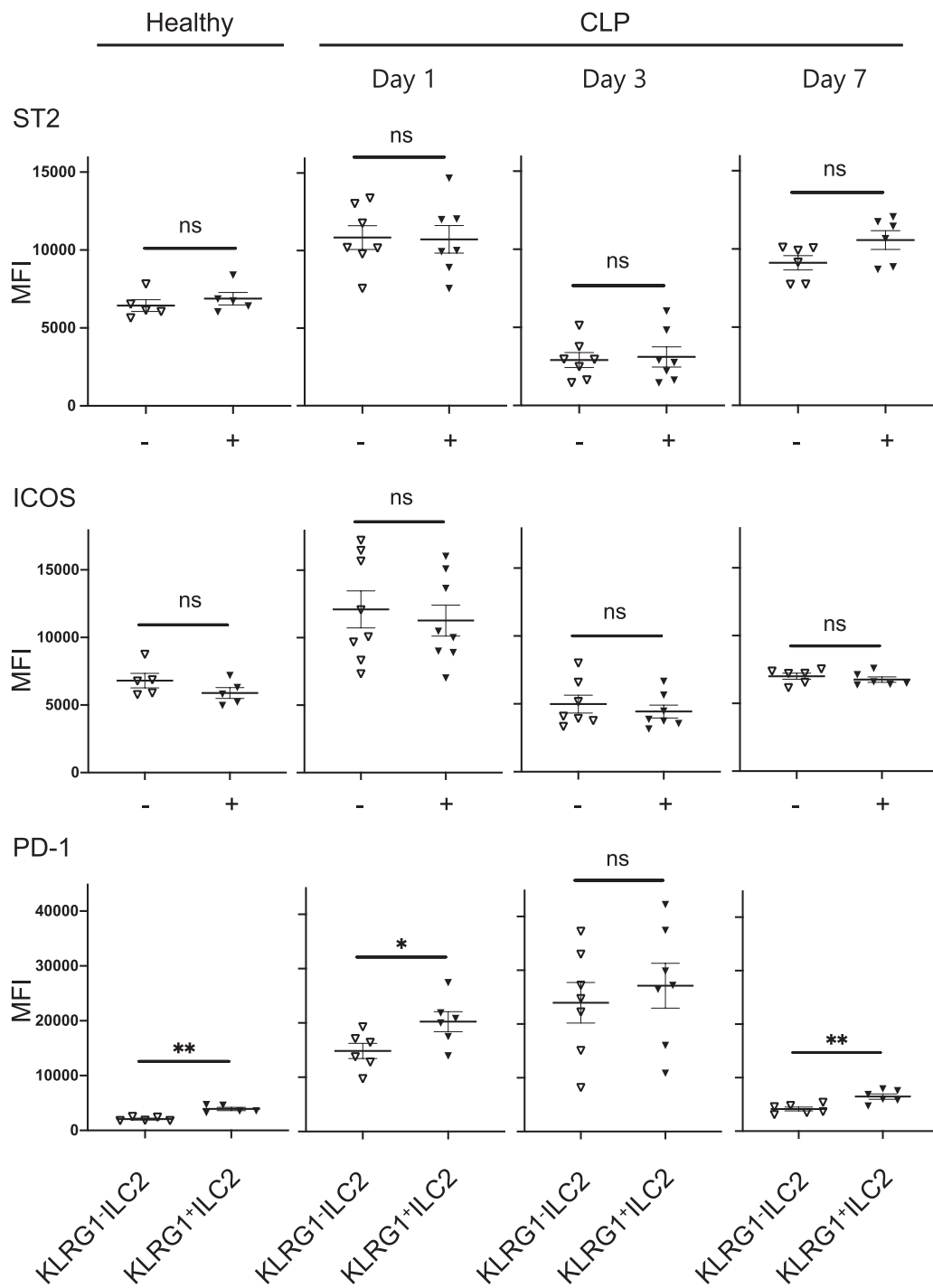
Fig. 8. **Phenotypic analysis of KLRG1$^+$ and KLRG1$^-$ ILC2s in the lung during sepsis.** MFI of surface marker (ST2 and ICOS, PD-1) phenotypes of KLRG1-negative and -positive ILC2s in the lungs of healthy and CLP mice. The data were evaluated using the Mann–Whitney test. Data represent the mean ± SEM. ns indicates not significant; KLRG1, killer cell lectin-like receptor G1; ILC2s, group 2 innate lymphoid cell; CLP, cecal ligation and puncture; MFI, mean fluorescence intensity; ICOS, inducible T-cell costimulator ; PD-1, programmed cell death 1. $^*P < 0.05$, $^{**}P < 0.01$.

were both reduced (Fig. 6, D and F), potentially perturbing the balance of the regulation, which resulted in the observed suppression of IL-13 production. Suppressed IL-13 production in the late phase of sepsis (i.e., day 7) could perturb the type 2 immune response needed for the resolution of inflammation, possibly explaining the more severe bodyweight loss observed in IL-33 KO septic mice compared with their WT counterparts

(Fig. 6, A and B). A previous study (9) that focused on the acute phase of CLP-induced sepsis in IL-33 KO mice showed increased lung edema, as evident by an Evans blue dye lung permeability assay conducted 24 h after CLP. This study pointed to the critical roles of ILC2 in the protection of endothelial cells. Unfortunately, we were unable to perform detailed pathohistological analysis of the septic IL-33 KO lungs
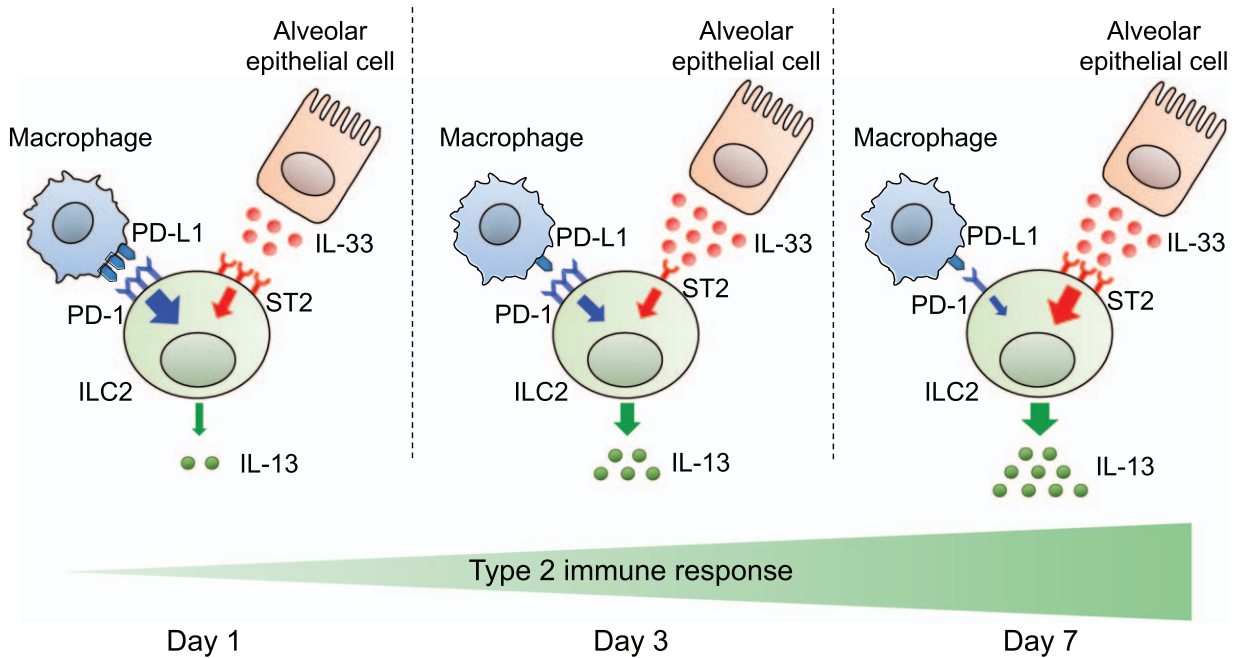
FIG. 9.   **A proposed model for IL-13-depdenent immune homeostasis in the septic lung regulated by the balance between the ST2-IL-33 axis and PD-1-PD-L1 axis in ILC2 s.** IL-33 released from injured lung epithelial cells elicits ST2-mediated stimulatory signals involving NF-kB and AP-1 activation, which promotes IL-13 production in ILC2 s (ST2-IL-33 axis). In contrast, PD-L1 upregulated in macrophages elicits PD-1-mediated inhibitory signals involving STAT5 inactivation, which suppresses IL-13 production in ILC2 s (PD-1-PD-L1 axis). The balance of signaling strengths between the ST2-IL-33 axis and the PD-1-PD-L1 axis would determine the levels of IL-13 production in ILC2 s, thereby remodeling immune homeostasis in the septic lung. ILC2 s indicates group 2 innate lymphoid cell; PD-1, programmed cell death 1.

due to technical problems. As our conventional IL-33 KO mice that lacked systemic IL-33 expression could compromise type 2 immune responses throughout the body, the more severe body-weight loss observed during sepsis may have resulted from sustained inflammation of not only the lung but also other organs.

We have demonstrated that the majority of ILC2 s in the septic lungs are an nILC2 subset that displays a tissue-resident phenotype and that responds to IL-33 (Fig. 5C). By contrast, in examining the septic lungs we observed barely any iILC2 subsets that displayed the migratory phenotype or responded to IL-25 (Fig. 5, B and C). Although the previous study showed that IL-25 treatment induced the migration of intestinal iILC2 to the lung (27), septic lungs expressed little IL-25 mRNA (Fig. 5D), which likely explains the lack of substantial iILC2 pulmonary accumulation (Fig. 5C). Therefore, the increase in ILC2 seen in the septic lung is likely to be induced by the proliferation of tissue-resident nILC2 s, rather than the migration of iILC2 to the lung from the intestine and/or other organs.

We sought to study KLRG1 signaling as an alternative inhibitory mechanism to regulate ILC2 in the septic lung, since KLRG1 is a C-type lectin inhibitory receptor that contains an immunoreceptor tyrosine-based inhibitory motif (16). Since the KLRG1⁻ ILC2 population is hardly detectable in the lungs of male mice (29), we therefore compared KLRG1⁻ and KLRG1⁺ ILC2 s in female mice. Unexpectedly, the production levels of type 2 cytokines by KLRG1⁻ ILC2 s were lower compared with those of KLRG1⁺ ILC2 s (Fig. 7). Additionally, we found that the levels of PD-1 expressed by KLRG1⁺ ILC2 s were significantly higher than those of KLRG1⁻ ILC2 s in both sham and

septic mice, except on day 3 after CLP (Fig. 8). Despite the higher levels of PD-1 expressed by KLRG1⁺ ILC2 s, there was a trend toward higher levels of IL-5 and IL-13 by KLRG1⁺ ILC2 s in septic mice. Furthermore, the levels of ST2 and ICOS did not significantly differ between the two groups (Fig. 8). These data suggest an intriguing possibility that KLRG1 may be involved in the activation, but not inactivation, of ILC2 s, which warrants further investigation. A possible drawback would be that we used only female mice, since the KLRG1⁻ ILC2 population is almost wholly absent from the lungs of male mice (29). Using female mice allowed us to readily study the roles of KLRG1 on ILC2 s in sepsis without using KLRG1 knockout mice (47). However, this could cause a potential bias, as previous studies have shown that lethality rates were lower in females than in males in the CLP mouse sepsis model (48). Further investigation would be required to exclude a potential gender bias and elucidate whether the differential susceptibility to sepsis in female and male CLP mice is attributable to the KLRG1⁻ ILC2 population.

Another possible drawback would be that we were unable to unravel the complex mechanisms underlying the interaction between the inhibition of IL-13 production and high PD-1 expression on ILC2 s due to the fact that most of our study was observational in nature. Despite this drawback, our study points to the possible inhibition of IL-13 production by PD-1 on ILC2 s, and provides new insights into the roles of ILC2 s in the pathophysiology of sepsis-induced lung inflammation. To study the physiological and pathological functions of ILC2, *in vivo* depletion of ILC2 has been achieved using either naturally occurring staggerer (Rora^{sg/sg}) and/or engineered conditionally

targeted (Rora^{fl/fl}) loss-of-function alleles of RORα, which is the key transcriptional factor specifically required for ILC2 differentiation (49, 50). Sub-lethally irradiated $Rag2^{-/-}Il2rg^{-/-}$ mice reconstituted with $Rora^{sg/sg}$ bone marrow cells ($Rora^{sg/sg}$ BMT mice) (49) and conditionally targeted $Rora^{fl/sg}$ mice inter-crossed with IL-7 receptor (IL-7R)-Cre ($Rora^{fl/sg}Il7r^{Cre}$) mice (50) have been shown to lack ILC2 (Supplemental Table 1, http://links.lww.com/SHK/B124). These engineered mutant mice lacking ILC2 have shown the following: a reduced susceptibility to an allergen (i.e., papain)-induced asthmatic reaction in the lung (49); an impaired ability to control helminth infection (50); and decreased IgA production in the gastrointestinal tracts (51). These research findings indicate that ILC2 s play a crucial role in orchestrating type 2 immunity, possibly through IL-13 and IL-5 secretion. However, it remains to be elucidated how sepsis-induced organ failures, particularly in the septic lung, would be affected in these engineered mutant mice lacking ILC2. Although we could not afford to use the mutant mice lacking ILC2 in this study, we have instead proposed an intriguing hypothesis: ILC2 plays the pivotal role in regulating IL-13-dependent immune homeostasis in the septic lung, which is controlled by the balance between the ST2-IL-33 axis and the PD-1-PD-L1 axis in ILC2 s (Fig. 9). The results of this study could contribute to future mechanistic investigations that would rigorously test this hypothesis using engineered mutant mice lacking ILC2.

In summary, we examined the temporal changes of cytokine expression and costimulatory/inhibitory molecules on ILC2 s from days 1 to 7 after CLP in the lung. Our major findings are as follows: Deregulation of IL-13 production in lung ILC2 s, which were predominately composed of the nILC2 subset, was induced by CLP. IL-13 production by ILC2 s was inhibited, and high PD-1 expression was clearly evident. IL-33 in the septic lung plays an important role in regulating the capacity of ILC2 to produce IL-13 via the modulation of ST2 and PD-1 expression and signaling. KLRG1 may be involved in the positive regulation of ILC2 functions. Although further studies are needed to elucidate the underlying molecular mechanism at work, our findings may contribute to filling the critical knowledge gap surrounding immune homeostasis in the septic lung that currently hampers the development of new therapeutic strategies for sepsis-associated ALI.
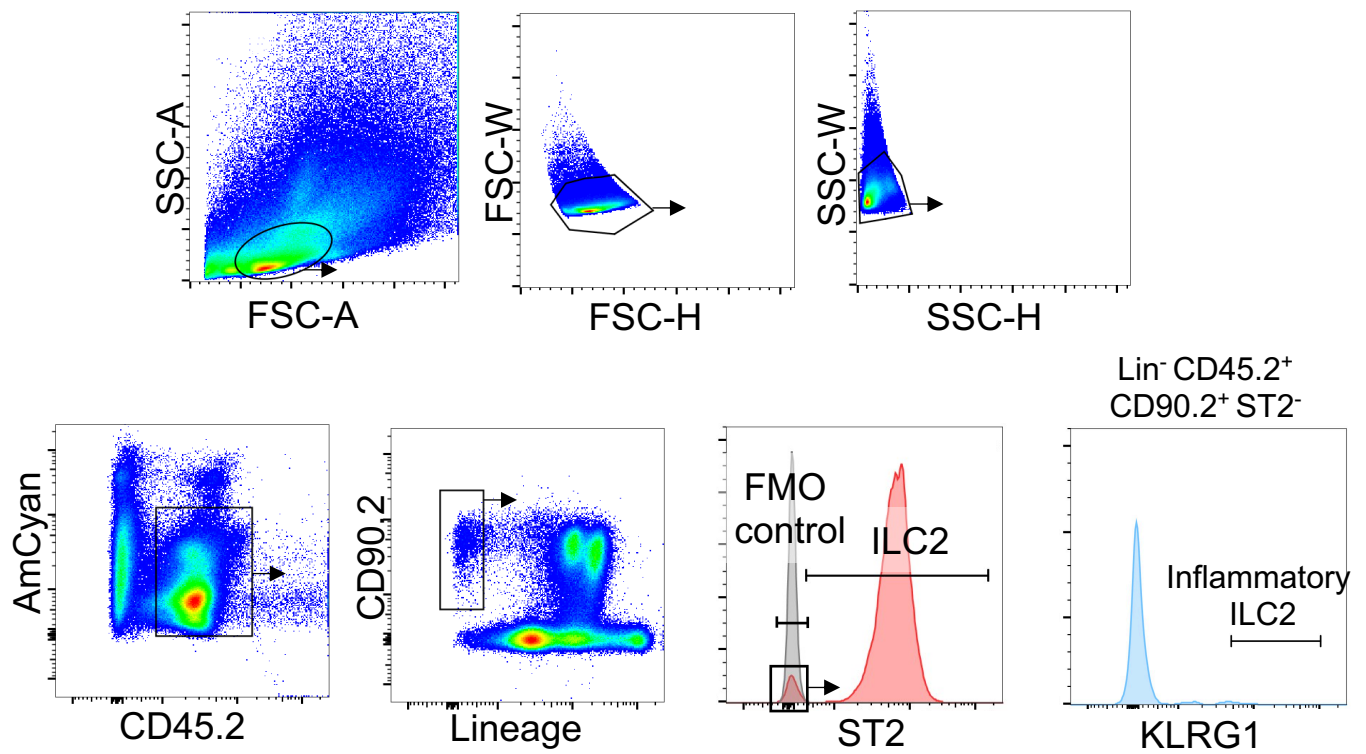
ACKNOWLEDGMENTS

REFERENCES

1. Vivier E, Artis D, Colonna M, Diefenbach A, Santo JP, Eberl G, Koyasu S, Locksley RM, McKenzie A, Mebius RE, et al.: Innate lymphoid cells: 10 years on. *Cell* 174(5):1054–1066, 2018.

2. Spits H, Santo JP: The expanding family of innate lymphoid cells: regulators and effectors of immunity and tissue remodeling. *Nat Immunol* 12(1):21–27, 2011.

3. Sonnenberg GF, Hepworth MR: Functional interactions between innate lymphoid cells and adaptive immunity. *Nat Rev Immunol* 19(10):599–613, 2019.

4. Castellanos JG, Longman RS: The balance of power: innate lymphoid cells in tissue inflammation and repair. *J Clin Invest* 129(7):2640–2650, 2019.

5. Singer M, Deutschman CS, Seymour C, Shankar-Hari M, Annane D, Bauer M, Bellomo R, Bernard GR, Chiche J-D, Coopersmith CM, et al.: The Third International Consensus Definitions for Sepsis and Septic Shock (Sepsis-3). *JAMA* 315(8):801–810, 2016.

6. Hudson LD, Steinberg KP: Epidemiology of acute lung injury and ARDS. *Chest* 116(1 suppl):74S–82S, 1999.

7. Moro K, Yamada T, Tanabe M, Takeuchi T, Ikawa T, Kawamoto H, Furusawa J-i, Ohtani M, Fujii H, Koyasu S: Innate production of TH2 cytokines by adipose tissue-associated c-Kit+Sca-1+ lymphoid cells. *Nature* 463(7280):540–544, 2010.

8. Salimi M, Barlow JL, Saunders SP, Xue L, Gutowska-Owsiak D, Wang X, Huang L-C, Johnson D, Scanlon ST, McKenzie A, et al.: A role for IL-25 and IL-33–driven type-2 innate lymphoid cells in atopic dermatitis. *J Exp Med* 210(13):2939–2950, 2013.

9. Lai D, Tang J, Chen L, Fan EK, Scott MJ, Li Y, Billiar TR, Wilson MA, Fang X, Shu Q, et al.: Group 2 innate lymphoid cells protect lung endothelial cells from pyroptosis in sepsis. *Cell Death Dis* 9(3):369, 2018.

10. Xu H, Xu J, Xu L, Jin S, Turnquist HR, Hoffman R, Loughran P, Billiar TR, Deng M: Interleukin-33 contributes to ILC2 activation and early inflammation-associated lung injury during abdominal sepsis. *Immunol Cell Biol* 96(9):935–947, 2018.

11. Krishack PA, Louviere TJ, Decker TS, Kuzel TG, Greenberg JA, Camacho DF, Hrusch CL, Sperling AI, Verhoef PA: Protection against Staphylococcus aureus bacteremia-induced mortality depends on ILC2 s and eosinophils. *JCI Insight* 4(6):e124168, 2019.

12. Nascimento DC, Melo PH, Pineros AR, Ferreira RG, Colon DF, Donate PB, Castanheira FV, Gozzi A, Czaikoski PG, Niedbala W, et al.: IL-33 contributes to sepsis-induced long-term immunosuppression by expanding the regulatory T cell population. *Nat Commun* 8:14919, 2017.

13. Maazi H, Patel N, Sankaranarayanan I, Suzuki Y, Rigas D, Soroosh P, Freeman GJ, Sharpe AH, Akbari O: ICOS:ICOS-ligand interaction is required for type 2 innate lymphoid cell function, homeostasis, and induction of airway hyperreactivity. *Immunity* 42(3):538–551, 2015.

14. Taylor S, Huang Y, Mallett G, Stathopoulou C, Felizardo TC, Sun M-A, Martin EL, Zhu N, Woodward EL, Elias MS, et al.: PD-1 regulates KLRG1+ group 2 innate lymphoid cells. *J Exp Med* 214(6):1663–1678, 2017.

15. Shindo Y, McDonough JS, Chang KC, Ramachandra M, Sasikumar PG, Hotchkiss RS: Anti-PD-L1 peptide improves survival in sepsis. *J Surg Res* 208:33–39, 2017.

16. Tessmer MS, Fugere C, Stevenaert F, Naidenko OV, Chong JH, Leclercq G, Brossay L: KLRG1 binds cadherins and preferentially associates with SHIP-1. *Int Immunol* 19(4):391–400, 2007.

17. Cyktor JC, Carruthers B, Stromberg P, Flano E, Pircher H, Turner J: Killer cell lectin-like receptor G1 deficiency significantly enhances survival after Mycobacterium tuberculosis infection. *Infect Immun* 81(4):1090–1099, 2013.

18. Oboki K, Ohno T, Kajiwara N, Arae K, Morita H, Ishii A, Nambu A, Abe T, Kiyonari H, Matsumoto K, et al.: IL-33 is a crucial amplifier of innate rather than acquired immunity. *Proc Natl Acad Sci U S A* 107(43):18581–18586, 2010.

19. Rittirsch D, Huber-Lang MS, Flierl MA, Ward PA: Immunodesign of experimental sepsis by cecal ligation and puncture. *Nat Protoc* 4(1):31–36, 2009.

20. Matute-Bello G, Downey G, Moore BB, Groshong SD, Matthay MA, Slutsky AS, Kuebler WM: An Official American Thoracic Society Workshop Report: features and measurements of experimental acute lung injury in animals. *Am J Respir Cell Mol Biol* 44(5):725–738, 2011.

21. Yin R, Tian F, Frankenberger B, de Angelis MH, Stoeger T: Selection and evaluation of stable housekeeping genes for gene expression normalization in carbon nanoparticle-induced acute pulmonary inflammation in mice. *Biochem Biophys Res Commun* 399(4):531–536, 2010.

22. Pichery M, Mirey E, Mercier P, Lefrancais E, Dujardin A, Ortega N, Girard JP: Endogenous IL-33 is highly expressed in mouse epithelial barrier tissues, lymphoid organs, brain, embryos, and inflamed tissues: in situ analysis using a novel Il-33-LacZ gene trap reporter strain. *J Immunol* 188(7):3488–3495, 2012.

23. Dong C, Juedes AE, Temann UA, Shresta S, Allison JP, Ruddle NH, Flavell RA: ICOS co-stimulatory receptor is essential for T-cell activation and function. *Nature* 409(6816):97–101, 2001.

24. Parry RV, Chemnitz JM, Frauwirth KA, Lanfranco AR, Braunstein I, Kobayashi SV, Linsley PS, Thompson CB, Riley JL: CTLA-4 and PD-1 receptors inhibit T-cell activation by distinct mechanisms. *Mol Cell Biol* 25(21):9543–9553, 2005.

25. Beldi-Ferchiou A, Lambert M, Dogniaux S, Vély F, Vivier E, Olive D, Dupuy S, Levasseur F, Zucman D, Lebbé C, et al.: PD-1 mediates functional exhaustion of activated NK cells in patients with Kaposi sarcoma. *Oncotarget* 7(45):72961–72977, 2016.

26. Huang Y, Paul WE: Inflammatory group 2 innate lymphoid cells. *Int Immunol* 28(1):23–28, 2016.

27. Huang Y, Mao K, Chen X, Sun MA, Kawabe T, Li W, Usher N, Zhu J, Urban JF Jr, Paul WE, et al.: S1P-dependent interorgan trafficking of group 2 innate lymphoid cells supports host defense. *Science* 359(6371):114–119, 2018.

28. Huang Y, Guo L, Qiu J, Chen X, Hu-Li J, Siebenlist U, Williamson PR, Urban JF Jr, Paul WE: IL-25-responsive, lineage-negative KLRG1(hi) cells are multi-potential 'inflammatory' type 2 innate lymphoid cells. *Nat Immunol* 16(2):161–169, 2015.

29. Kadel S, Ainsua-Enrich E, Hatipoglu I, Turner S, Singh S, Khan S, Kovats S: A major population of functional KLRG1(−) ILC2 s in female lungs contributes to a sex bias in ILC2 numbers. *Immunohorizons* 2(2):74–86, 2018.

30. Cayrol C, Girard JP: IL-33: an alarmin cytokine with crucial roles in innate immunity, inflammation and allergy. *Curr Opin Immunol* 31:31–37, 2014.

31. Matsukawa A, Hogaboam CM, Lukacs NW, Lincoln PM, Evanoff HL, Strieter RM, Kunkel SL: Expression and contribution of endogenous IL-13 in an experimental model of sepsis. *J Immunol* 164(5):2738–2744, 2000.

32. Kim J, Chang Y, Bae B, Sohn KH, Cho SH, Chung DH, Kang HR, Kim HY: Innate immune crosstalk in asthmatic airways: innate lymphoid cells coordinate polarization of lung macrophages. *J Allergy Clin Immunol* 143(5):1769.e11–1782.e11, 2019.

33. Tang L, Zhang H, Wang C, Li H, Zhang Q, Bai J: M2A and M2C macrophage subsets ameliorate inflammation and fibroproliferation in acute lung injury through interleukin 10 pathway. *Shock* 48(1):119–129, 2017.

34. Zhang Y, Li J, Lou J, Zhou Y, Bo L, Zhu J, Zhu K, Wan X, Cai Z, Deng X: Upregulation of programmed death-1 on T cells and programmed death ligand-1 on monocytes in septic shock patients. *Crit Care* 15(1):R70, 2011.

35. Brahmamdam P, Inoue S, Unsinger J, Chang KC, McDunn JE, Hotchkiss RS: Delayed administration of anti-PD-1 antibody reverses immune dysfunction and improves survival during sepsis. *J Leukoc Biol* 88(2):233–240, 2010.

36. Zhang Y, Zhou Y, Lou J, Li J, Bo L, Zhu K, Wan X, Deng X, Cai Z: PD-L1 blockade improves survival in experimental sepsis by inhibiting lymphocyte apoptosis and reversing monocyte dysfunction. *Crit Care* 14(6):R220, 2010.

37. Schmitz J, Owyang A, Oldham E, Song Y, Murphy E, McClanahan TK, Zurawski G, Moshrefi M, Qin J, Li X, et al.: IL-33, an interleukin-1-like cytokine that signals via the IL-1 receptor-related protein ST2 and induces T helper type 2-associated cytokines. *Immunity* 23(5):479–490, 2005.

38. Kim J, Kim W, Moon UJ, Kim HJ, Choi HJ, Sin JI, Park NH, Cho HR, Kwon B: Intratumorally establishing type 2 innate lymphoid cells blocks tumor growth. *J Immunol* 196(5):2410–2423, 2016.

39. Cardoso V, Chesné J, Ribeiro H, García-Cassani B, Carvalho T, Bouchery T, Shah K, Barbosa-Morais NL, Harris N, Veiga-Fernandes H: Neuronal regulation of type 2 innate lymphoid cells via neuromedin U. *Nature* 549(7671):277–281, 2017.

40. Sharpe AH, Pauken KE: The diverse functions of the PD1 inhibitory pathway. *Nat Rev Immunol* 18(3):153–167, 2018.

41. Oldenhove G, Boucquey E, Taquin A, Acolty V, Bonetti L, Ryffel B, Le Bert M, Englebert K, Boon L, Moser M: PD-1 is involved in the dysregulation of type 2 innate lymphoid cells in a murine model of obesity. *Cell Rep* 25(8):2053.e4–2060.e4, 2018.

42. Nussbaum JC, Van Dyken SJ, Von Moltke J, Cheng LE, Mohapatra A, Molofsky AB, Thornton EE, Krummel MF, Chawla A, Liang H-E, et al.: Type 2 innate lymphoid cells control eosinophil homeostasis. *Nature* 502(7470):245–248, 2013.

43. Gibbings SL, Thomas SM, Atif SM, McCubbrey AL, Desch AN, Danhorn T, Leach SM, Bratton DL, Henson PM, Janssen WJ, et al.: Three unique interstitial macrophages in the murine lung at steady state. *Am J Respir Cell Mol Biol* 57(1):66–76, 2017.

44. Lüthi AU, Cullen SP, McNeela EA, Duriez PJ, Afonina IS, Sheridan C, Brumatti G, Taylor RC, Kersse K, Vandenabeele P, et al.: Suppression of interleukin-33 bioactivity through proteolysis by apoptotic caspases. *Immunity* 31(1):84–98, 2009.

45. Sun C, Mezzadra R, Schumacher TN: Regulation and function of the PD-L1 checkpoint. *Immunity* 48(3):434–452, 2018.

46. Oyesola OO, Duque C, Huang LC, Larson EM, Fruh SP, Webb LM, Peng SA, Tait Wojno ED: The Prostaglandin D2 receptor CRTH2 promotes IL-33-induced ILC2 accumulation in the lung. *J Immunol* 204(4):1001–1011, 2020.

47. Gründemann C, Schwartzkopff S, Koschella M, Schweier O, Peters C, Voehringer D, Pircher H: The NK receptor KLRG1 is dispensable for virus-induced NK and CD8+ T-cell differentiation and function in vivo. *Eur J Immunol* 40(5):1303–1314, 2010.

48. Zellweger R, Wichmann MW, Ayala A, Stein S, DeMaso CM, Chaudry IH: Females in proestrus state maintain splenic immune functions and tolerate sepsis better than males. *Crit Care Med* 25(1):106–110, 1997.

49. Halim TY, MacLaren A, Romanish MT, Gold MJ, McNagny KM, Takei F: Retinoic-acid-receptor-related orphan nuclear receptor alpha is required for natural helper cell development and allergic inflammation. *Immunity* 37(3):463–474, 2012.

50. Oliphant CJ, Hwang YY, Walker JA, Salimi M, Wong SH, Brewer JM, Englezakis A, Barlow JL, Hams E, Scanlon ST, et al.: MHCII-mediated dialog between group 2 innate lymphoid cells and CD4(+) T cells potentiates type 2 immunity and promotes parasitic helminth expulsion. *Immunity* 41(2):283–295, 2014.

51. Satoh-Takayama N, Kato T, Motomura Y, Kageyama T, Taguchi-Atarashi N, Kinoshita-Daitoku R, Kuroda E, Di Santo JP, Mimuro H, Moro K, et al.: Bacteria-induced group 2 innate lymphoid cells in the stomach provide immune protection through induction of IgA. *Immunity* 52(4):635.e4–649.e4, 2020

Fig. S1
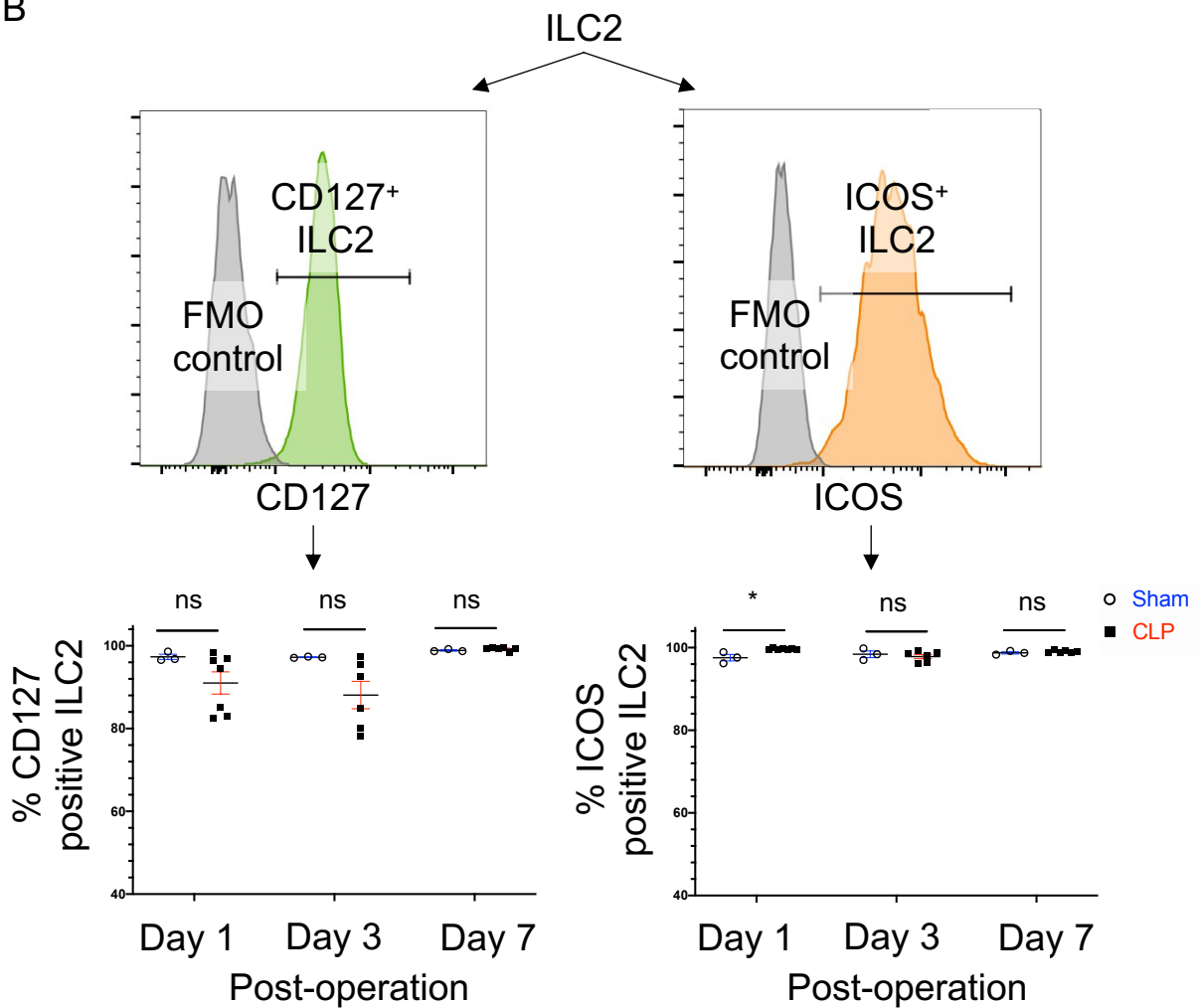
A

B

Fig. S2

CLP

	Day 1	Day 3	Day 7

IL-5

51.6±12.9% 22.5±4.2% 64.6±3.9%

IL-13

9.9±1.8% 7.7±3.6% 27.6±5.0%

FSC

Healthy

IL-5

41.9±12.6%

IL-13

19.5±3.1%

FSC

Sham

	Day 1	Day 3	Day 7

IL-5

62.5±18.5% 30.5±20% 60.0±15.8%

IL-13

25.0±0.7% 12.3±6.7% 20.2±4.1%

FSC

Fig. S3

FMO
control

ILC2

% of Max

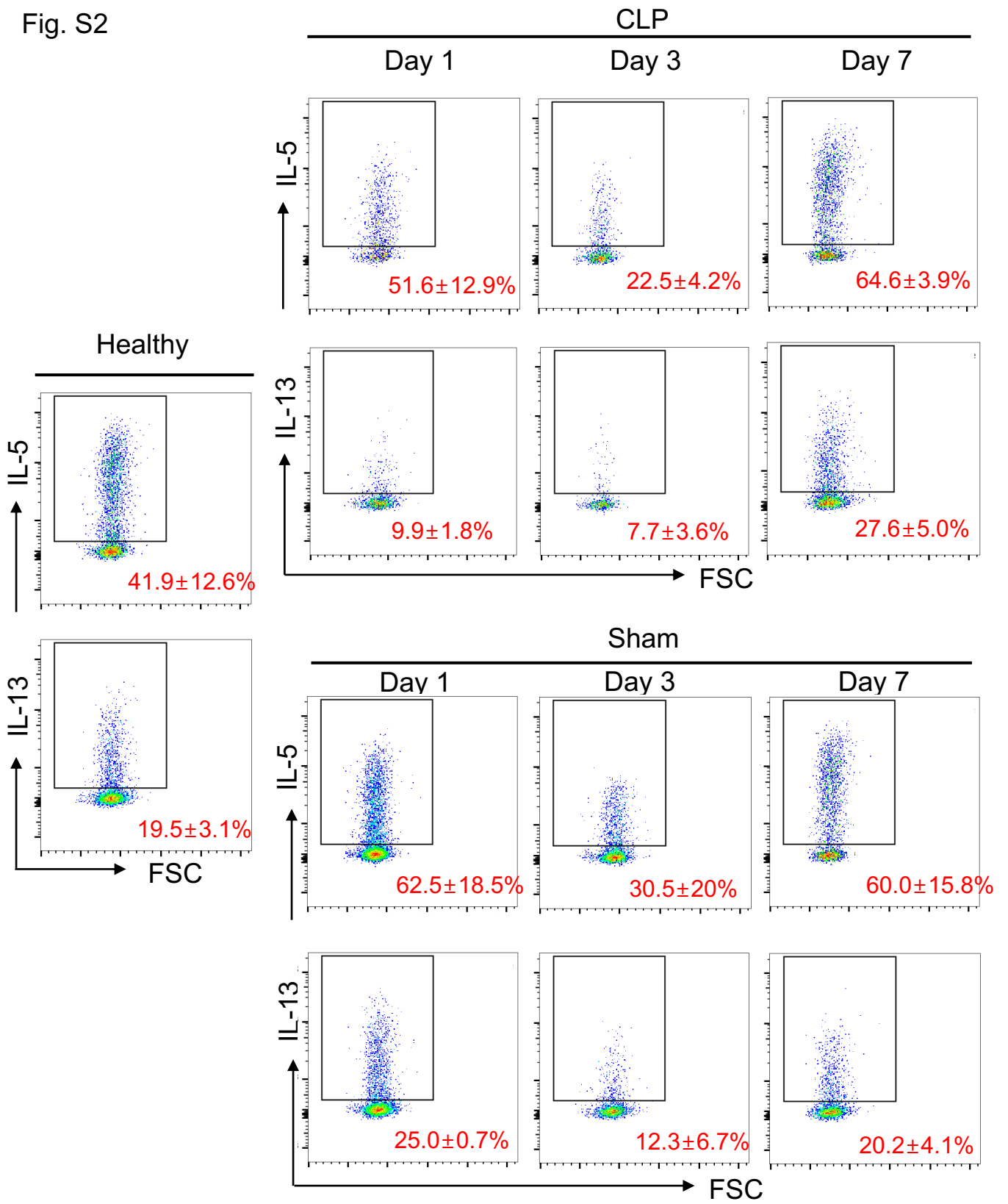ST2

KLRG1⁻ ILC2   KLRG1⁺ ILC2
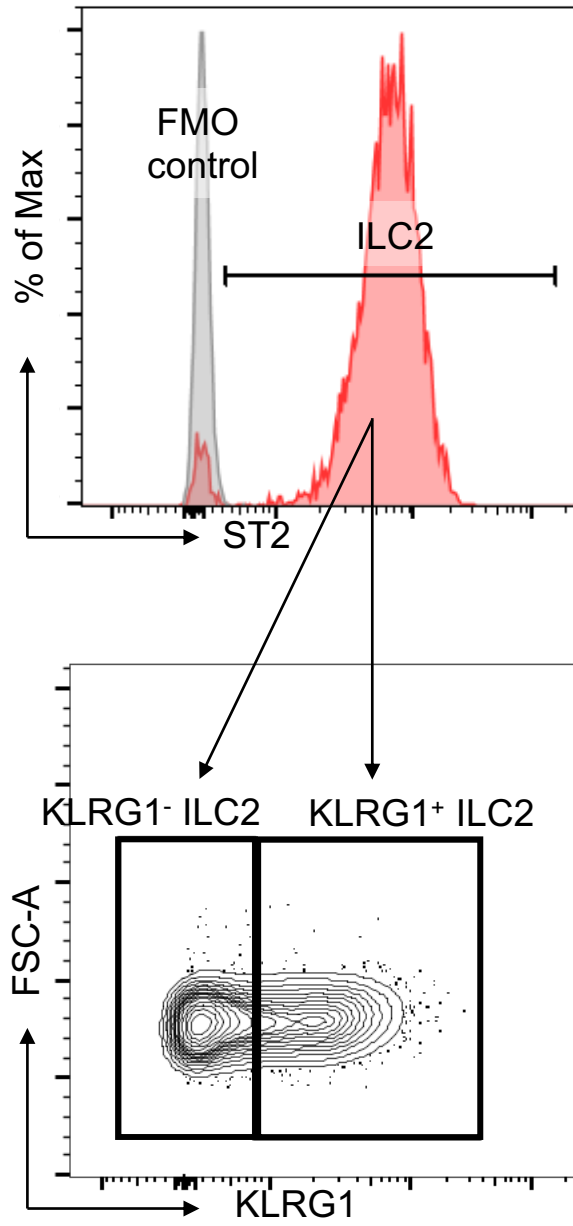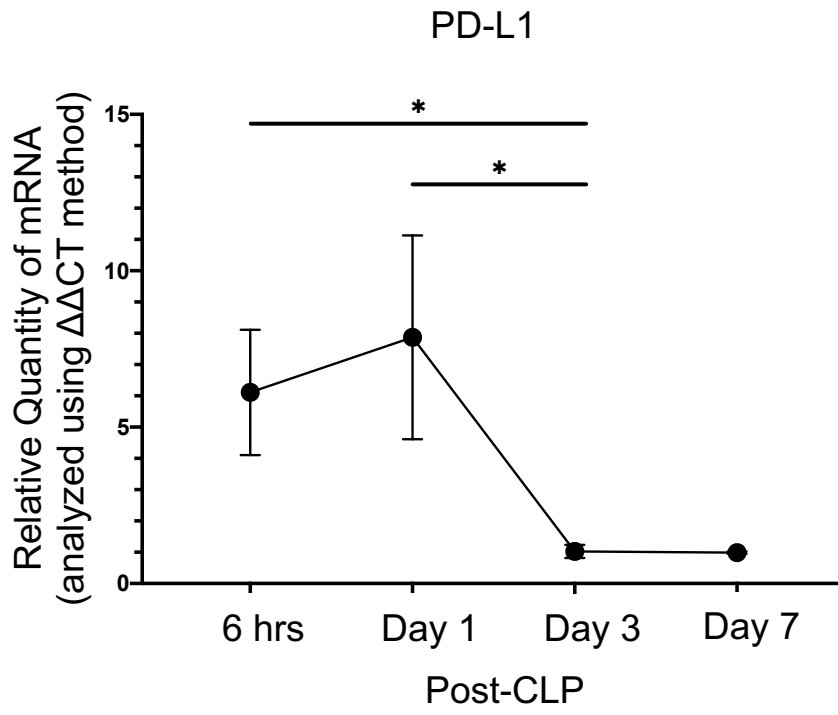
FSC-A

KLRG1

Fig. S4

PD-L1

Supplemental Table 1. a list of previous reports that studied engineered mutant mice lacking ILC2

A. *Rora*$^{sg/sg}$ BMT mice

Author, year	Organs studied	Disease model	Remarks
Halim, 2012	Lung and gut	Papain-induced asthma model	Even in the presence of intact Th2 cells, ILC2s are required for the inflammatory response to allergens.
Halim, 2014	Lung and LNs	Papain-induced asthma model	ILC2-derived IL-13 promotes the migration of DCs to LNs, thereby priming naive T cells to differentiate into Th2 cells.
Gold, 2014	Lung	House dust mite-induced asthma model	Significant reduction in BAL eosinophils in ILC2-deficient mice
Li, 2014	Bile duct	Biliary injury model	ILC2-derived IL-13 promotes epithelial repair.
Halim, 2016	Lung and skin	Papain-induced asthma model	ILC2s induce DCs to promote memory Th2 function.
Xu, 2017	Lung	Helminth-infected mouse model	Eocinophil accumulation was reduced in ILC2-deficient mice.
Yasuda, 2018	Lung	Hemorrhagic shock model	IL-33, ILC2 deficient, or IL-5 neutralization leads to reduced lung injury scores.
Imai, 2019	Skin	Atopic dermatitis-like model	Atopic dermatitis-like inflammation is impaired in ILC2-deficient mice.
Satoh-Takayama, 2020	Stomach	*H. pylori*-infected mouse model	ILC2-derived IL-5 upregulates the B-cell IgA response in the stomach, leading to protection against bacterial exposure.

B. *Rora*^{fl/sg}*Il7r*^{Cre} mice

Author, year	Organs studied	Disease model	Remarks
Oliphant, 2014	Gut	Helminth-infected mouse model	ILC2 ablation leads to impaired type 2 response against helminth infection.
Walker, 2015	Gut	Helminth-infected mouse model	Bcl11b is essential for ILC2-mediated function against helminth infection.
Halim, 2016	Lung and skin	Papain-induced asthma model	ILC2s induce DCs to promote memory Th2 function.
Hams, 2016	Kedney	Acute kideny injury model	The absence of ILC2s does not alter the severity of the renal injury model.
Newland, 2017	Adipose tissue	High-fat diet mouse model	ω1-induced ILC2s are needed for weight loss and improve glucose tolerance.
Halim, 2018	Lung and mesenteric LNs	Papain-induced asthma model Helminth-infected mouse model	CD4$^+$ T cells in the mLN and lung IgE concentrations are reduced in ILC2-deficient mice.
Rafei-Shamsabadi, 2018	Skin	Allergic contact dermatitis model	ILC2s act as negative regulators in type 1 immune response.
Donovan, 2019	Lung	Cigarette smoke exposure in mice	There was decreased collagen deposition in the lung following cigarette exposure in a study of ILC2 deficiency.
Schwartz, 2019	Skin	Skin inflammation model (spontaneously induced by Filaggrin-mutant mice)	Chronic dermatitis does not improve with ILC2 deficiency.
Cameron, 2019	Aorta	Atherosclerosis model (induced by low-density lipoprotein receptor-dificient mice)	ILC2-deficiency exacerbates atherosclerosis.
Moral, 2020	Pancrease	Pancreatic cancer model	The number of DCs in the tumor is lower in ILC2-deficient mice.

DCs: dendritic cells, LNs: lympho nodes, BAL: bronchoalveolar lavage

References

Cameron, G.J.M., Cautivo, K.M., Loering, S., Jiang, S.H., Deshpande, A.V., Foster, P.S., McKenzie, A.N.J., Molofsky, A.B., Hansbro, P.M., and Starkey, M.R. (2019). Group 2 Innate Lymphoid Cells Are Redundant in Experimental Renal Ischemia-Reperfusion Injury. Front Immunol *10*, 826.

Donovan, C., Starkey, M.R., Kim, R.Y., Rana, B.M.J., Barlow, J.L., Jones, B., Haw, T.J., Mono Nair, P., Budden, K., Cameron, G.J.M.*, et al.* (2019). Roles for T/B lymphocytes and ILC2s in experimental chronic obstructive pulmonary disease. J Leukoc Biol *105*, 143-150.

Gold, M.J., Antignano, F., Halim, T.Y., Hirota, J.A., Blanchet, M.R., Zaph, C., Takei, F., and McNagny, K.M. (2014). Group 2 innate lymphoid cells facilitate sensitization to local, but not systemic, TH2-inducing allergen exposures. J Allergy Clin Immunol *133*, 1142-1148.

Halim, T.Y., Hwang, Y.Y., Scanlon, S.T., Zaghouani, H., Garbi, N., Fallon, P.G., and McKenzie, A.N. (2016). Group 2 innate lymphoid cells license dendritic cells to potentiate memory TH2 cell responses. Nat Immunol *17*, 57-64.

Halim, T.Y., MacLaren, A., Romanish, M.T., Gold, M.J., McNagny, K.M., and Takei, F. (2012). Retinoic-acid-receptor-related orphan nuclear receptor alpha is required for natural helper cell development and allergic inflammation. Immunity *37*, 463-474.

Halim, T.Y., Steer, C.A., Matha, L., Gold, M.J., Martinez-Gonzalez, I., McNagny, K.M., McKenzie, A.N., and Takei, F. (2014). Group 2 innate lymphoid cells are critical for the initiation of adaptive T helper 2 cell-mediated allergic lung inflammation. Immunity *40*, 425-435.

Halim, T.Y.F., Rana, B.M.J., Walker, J.A., Kerscher, B., Knolle, M.D., Jolin, H.E., Serrao, E.M., Haim-Vilmovsky, L., Teichmann, S.A., Rodewald, H.R.*, et al.* (2018). Tissue-Restricted Adaptive Type 2 Immunity Is Orchestrated by Expression of the Costimulatory Molecule OX40L on Group 2 Innate Lymphoid Cells. Immunity *48*, 1195-1207 e1196.

Hams, E., Bermingham, R., Wurlod, F.A., Hogan, A.E., O'Shea, D., Preston, R.J., Rodewald, H.R., McKenzie, A.N., and Fallon, P.G. (2016). The helminth T2 RNase omega1 promotes metabolic homeostasis in an IL-33- and group 2 innate lymphoid cell-dependent mechanism. FASEB J *30*, 824-835.

Imai, Y., Yasuda, K., Nagai, M., Kusakabe, M., Kubo, M., Nakanishi, K., and Yamanishi, K. (2019). IL-33-Induced Atopic Dermatitis-Like Inflammation in Mice Is Mediated by Group 2 Innate Lymphoid Cells in Concert with Basophils. J Invest Dermatol *139*, 2185-2194 e2183.

Li, J., Razumilava, N., Gores, G.J., Walters, S., Mizuochi, T., Mourya, R., Bessho, K., Wang, Y.H., Glaser, S.S., Shivakumar, P.*, et al.* (2014). Biliary repair and carcinogenesis are mediated by IL-33-dependent cholangiocyte proliferation. J Clin Invest *124*, 3241-3251.

Moral, J.A., Leung, J., Rojas, L.A., Ruan, J., Zhao, J., Sethna, Z., Ramnarain, A., Gasmi, B., Gururajan, M., Redmond,

D*., et al.* (2020). ILC2s amplify PD-1 blockade by activating tissue-specific cancer immunity. Nature *579*, 130-135.

Newland, S.A., Mohanta, S., Clement, M., Taleb, S., Walker, J.A., Nus, M., Sage, A.P., Yin, C., Hu, D., Kitt, L.L*., et al.* (2017). Type-2 innate lymphoid cells control the development of atherosclerosis in mice. Nat Commun *8*, 15781.

Oliphant, C.J., Hwang, Y.Y., Walker, J.A., Salimi, M., Wong, S.H., Brewer, J.M., Englezakis, A., Barlow, J.L., Hams, E., Scanlon, S.T*., et al.* (2014). MHCII-mediated dialog between group 2 innate lymphoid cells and CD4(+) T cells potentiates type 2 immunity and promotes parasitic helminth expulsion. Immunity *41*, 283-295.

Rafei-Shamsabadi, D.A., van de Poel, S., Dorn, B., Kunz, S., Martin, S.F., Klose, C.S.N., Arnold, S.J., Tanriver, Y., Ebert, K., Diefenbach, A*., et al.* (2018). Lack of Type 2 Innate Lymphoid Cells Promotes a Type I-Driven Enhanced Immune Response in Contact Hypersensitivity. J Invest Dermatol *138*, 1962-1972.

Satoh-Takayama, N., Kato, T., Motomura, Y., Kageyama, T., Taguchi-Atarashi, N., Kinoshita-Daitoku, R., Kuroda, E., Di Santo, J.P., Mimuro, H., Moro, K*., et al.* (2020). Bacteria-Induced Group 2 Innate Lymphoid Cells in the Stomach Provide Immune Protection through Induction of IgA. Immunity *52*, 635-649 e634.

Schwartz, C., Moran, T., Saunders, S.P., Kaszlikowska, A., Floudas, A., Bom, J., Nunez, G., Iwakura, Y., O'Neill, L., Irvine, A.D*., et al.* (2019). Spontaneous atopic dermatitis in mice with a defective skin barrier is independent of ILC2 and mediated by IL-1beta. Allergy *74*, 1920-1933.

Walker, J.A., Oliphant, C.J., Englezakis, A., Yu, Y., Clare, S., Rodewald, H.R., Belz, G., Liu, P., Fallon, P.G., and McKenzie, A.N. (2015). Bcl11b is essential for group 2 innate lymphoid cell development. J Exp Med *212*, 875-882.

Xu, J., Guardado, J., Hoffman, R., Xu, H., Namas, R., Vodovotz, Y., Xu, L., Ramadan, M., Brown, J., Turnquist, H.R*., et al.* (2017). IL33-mediated ILC2 activation and neutrophil IL5 production in the lung response after severe trauma: A reverse translation study from a human cohort to a mouse trauma model. PLoS Med *14*, e1002365.

Yasuda, K., Adachi, T., Koida, A., and Nakanishi, K. (2018). Nematode-Infected Mice Acquire Resistance to Subsequent Infection With Unrelated Nematode by Inducing Highly Responsive Group 2 Innate Lymphoid Cells in the Lung. Front Immunol *9*, 2132.